Journal of Environmental Management 373 (2025) 123586

Contents lists available at ScienceDirect

Journal of Environmental Management

journal homepage: www.elsevier.com/locate/jenvman

Research article

Sulfur-functionalized sawdust biochar for enhanced cadmium adsorption and environmental remediation: A multidisciplinary approach and density functional theory insights

M.M.M. Ahmed [a,b], Chih-Hao Liao [a,b], S. Venkatesan [c], Yu-Ting Liu [a,b], Yu-Min Tzou [a,b,**], Shih-Hao Jien [a,b,***], Ming-Chang Lin [d], Yi-Cheng Hsieh [e], Ahmed I. Osman [f,*]

[a] Department of Soil and Environmental Sciences, National Chung Hsing University, 145 Xingda Rd., Taichung, 40227, Taiwan
[b] Innovation and Development Center of Sustainable Agriculture, National Chung Hsing University, 145 Xingda Rd., Taichung, 40227, Taiwan
[c] Department of Chemistry, School of Science and Humanities, Vignan's Foundation for Science, Technology and Research, Vadlamudi, Guntur, Andhra Pradesh, 522 213, India
[d] Department of Applied Chemistry, National Yang Ming Chiao Tung University, Hsinchu, 30010, Taiwan
[e] Office of the Texas State Chemist, Texas A&M AgriLife Research, Texas A&M University System, College Station, TX, 77843, USA
[f] School of Chemistry and Chemical Engineering, David Keir Building, Queen's University Belfast, Stranmillis Road, Belfast, BT9 5AG, Northern Ireland, UK

ARTICLE INFO

Keywords:
Sulfur doped
Biochar
Cadmium adsorption
Water purification
DFT
Circular bioeconomy

ABSTRACT

Pristine biochar typically exhibits limited capacity for heavy metal adsorption due to its inadequate pore development and insufficient surface functionality. This study introduces an innovative chemical strategy to enhance the surface of sawdust biochar with sulfur-based functional groups (C=S, C-S, S-S, S^{2-}, S-H, $-SO_3^{2-}$, $-SO_4^{2-}$) to significantly improve cadmium (Cd) adsorption. Sulfur-doping using H_2SO_4, Na_2S, and $Na_2S_2O_3$ markedly increased the sulfur content from 0.11% (pristine) to 2.81% (H_2SO_4), 0.57% (Na_2S), and 13.27% ($Na_2S_2O_3$). Characterization techniques such as SEM-EDS, FTIR, and XPS confirmed the successful incorporation of sulfur moieties and additional oxygen-containing groups, improving surface functionality. The Cd adsorption capacity of S-modified biochar increased by 4.8–9.0 times compared to pristine biochar, with peak values of 39.38, 20.84, and 34.14 mg g^{-1} for H_2SO_4, Na_2S, and $Na_2S_2O_3$-modified biochar, respectively. The equilibrium time was significantly reduced from 4 h (pristine) to 5–10 min (S-modified). The enhanced Cd adsorption was attributed to the synergistic interplay of electrostatic attraction, cadmium-π electron interactions, complexation, and ion exchange mechanisms, facilitated by the presence of oxygen and sulfur functional groups. Density Functional Theory (DFT) calculations showed that sulfur doping modulated the electronic properties of the biochar-Cd systems, narrowing the band gap and enhancing the Cd-O bonds, thereby improving the Cd adsorption performance. Additionally, the binding energies of the S-modified biochar-Cd complex were found to be more stable compared to those before Cd adsorption. This study demonstrates that both oxygen and sulfur-functionalized sawdust biochar is an effective and eco-friendly adsorbent for Cd removal, highlighting the significance of tailored surface modifications to augment biochar's reactivity and affinity towards specific contaminants. The developed material offers a sustainable and scalable solution for Cd removal from aqueous environments, contributing to advanced water treatment technologies and environmental remediation strategies.

1. Introduction

Rapid industrialization has significantly increased the discharge of industrial wastewater containing various organic and inorganic toxic substances, posing severe ecological threats and risks to human health. Among these pollutants, heavy metals, particularly cadmium (Cd), are of major concern due to their high toxicity, mobility, and bioavailability (Khin et al., 2012; Sovacool et al., 2024). The United States

* Corresponding author.
** Corresponding author. Department of Soil and Environmental Sciences, 145 Xingda Rd., Taichung, 40227, Taiwan, Taiwan.
*** Corresponding author. Department of Soil and Environmental Sciences, 145 Xingda Rd., Taichung, 40227, Taiwan, Taiwan.
E-mail addresses: ymtzou@dragon.nchu.edu.tw (Y.-M. Tzou), shjien@nchu.edu.tw (S.-H. Jien), aosmanahmed01@qub.ac.uk (A.I. Osman).

https://doi.org/10.1016/j.jenvman.2024.123586
Received 20 August 2024; Received in revised form 4 November 2024; Accepted 1 December 2024

Environmental Protection Agency (EPA) lists Cd as a priority pollutant and classifies it as a carcinogenic chemical (Wang et al., 2007). The primary sources of Cd in the environment include mining and smelting activities and industrial effluents from electroplating and metal processing industries. To purify industrial wastewater and recycle limited water resources, various techniques such as chemical precipitation (Ostermeyer et al., 2021), membrane filtration, adsorption (Kim et al., 2022), ion exchange (Huang et al., 2020), and electrochemical treatment (Alkhadra et al., 2022) have been employed for Cd removal. Among these methods, adsorption has gained significant attention due to its simplicity, cost-effectiveness, and advantages, such as the ease of adsorbent production, recovery, and reusability (Majumder et al., 2023).

Biochar, a carbon-rich material derived from the pyrolysis of biomass (Liu et al., 2019; Kurniawan et al., 2023), has emerged as a versatile and sustainable solution for addressing environmental challenges (Lee et al., 2010). It has gained widespread attention not only for its effectiveness in addressing heavy metal issues but also for its environmentally friendly nature, being derived from agricultural residues (Khan et al., 2023; Osman et al., 2023a). Researchers have explored various biochar materials derived from agricultural residues such as wheat straw, tobacco dust, pine shavings, rice husks, bean pods, and almond shells for metal adsorption (Osman et al., 2023b; Kainth et al., 2024). Among these, sawdust (i.e., wood dust) is a promising feedstock for biochar production due to its high cellulose, hemicellulose, and lignin content, which, upon pyrolysis, provide a structure with numerous binding sites for metals (Tyagi and Anand, 2023). Additionally, converting these agricultural wastes into biochar is a viable and convenient approach to waste management (Chaubey et al., 2024). Biochar is a multifunctional material that can be used for carbon sequestration (Luo et al., 2023), land reclamation, pollutant immobilization, and soil fertility enhancement (Geissler and Maravelias, 2022). Its production helps reduce greenhouse gas emissions by capturing carbon in a stable form, thus contributing to climate change mitigation as an effective negative carbon technology (Cowie et al., 2024). Furthermore, biochar's porous structure and high surface area make it effective in retaining nutrients and improving soil health, thereby supporting sustainable agricultural practices (Cho et al., 2020; Lin et al., 2023). Hence, using biochar addresses heavy metal contamination in water and soil, promotes the recycling of agricultural residues, and supports circular economy principles and sustainable resource management (Osman et al., 2022; Li et al., 2023).

Biochar primarily comprises aliphatic and aromatic compounds with surface functional groups that facilitate chemical adsorption reactions with heavy metals through complexation, precipitation, and ion exchange processes (Huangmee et al., 2024). However, the adsorption capacity of biochar for heavy metals is often limited by constraints imposed by its surface pore structures, particularly those produced at lower carbonized temperatures or by the lower affinities of oxygen-containing functional groups to soft Lewis acids like Cd (Chen et al., 2022; Yuan et al., 2023). To enhance the Cd adsorption capacity of biochar, chemical modifications can be performed to enrich the surface functional groups with Lewis bases, such as sulfur (S) (Chen et al., 2020b). Since Cd is a soft Lewis acid, introducing sulfur-containing functional groups onto the biochar surface through modification can be expected to significantly enhance its adsorption capacity (Zhu et al., 2020a). This enhancement is due to the strong affinity of these sulfur groups towards soft Lewis acids like Cd, enabling robust interactions that facilitate adsorption (Fawzy et al., 2022; Amalina et al., 2024).

While numerous studies have explored sulfur-modified adsorbents for heavy metal adsorption, particularly for mercury (Hua et al., 2020), research on using sulfur-containing compounds to enhance cadmium (Cd) removal through biochar modification remains limited. This study aims to address this gap by modifying biochar using commonly available sulfur-containing compounds and examining the Cd adsorption capacities in aqueous solutions, both before and after modification. We carefully selected three sulfur-containing compounds—H_2SO_4 (96%), Na_2S, and $Na_2S_2O_3$—to modify sawdust-derived biochar for enhanced Cd adsorption. These compounds represent a broad range of sulfur species and oxidation states, from highly oxidized (SO_4^{2-}) to reduced (S^{2-}) forms, enabling a comprehensive investigation into the role of sulfur in Cd adsorption. Each compound provides unique surface modification capabilities: H_2SO_4 facilitates acid activation and sulfur doping (Zhao et al., 2010), Na_2S promotes the formation of metal sulfides and introduces reduced sulfur species (Bian et al., 2016), while $Na_2S_2O_3$ incorporates thiosulfate groups, offering an intermediate oxidation state (Chen et al., 2010). These compounds extend across a wide pH range, allowing us to assess the critical influence of pH during the modification process. Moreover, they are cost-effective and relatively safe to handle, making them viable for potential large-scale applications. Recent studies (Zhang et al., 2023a, 2023b; Zhao et al., 2024) have demonstrated their effectiveness in heavy metal adsorption, supporting the foundation for our research. By utilizing these three distinct sulfur-containing compounds, we aim to illustrate the complex relationships between sulfur species, oxidation states, and modification conditions in determining biochar's Cd adsorption capacity. This approach aligns with our broader objective of optimizing biochar modifications for effective and sustainable heavy metal remediation in environmental applications. Our methodology includes analyzing the incorporation of sulfur-containing functional groups using elemental analysis, SEM, FTIR, and XPS to estimate Cd immobilization capacity and interpret adsorption mechanisms. Additionally, we employed density functional theory (DFT) calculations to provide theoretical insights into the reaction mechanisms and predict the stability of the [biochar-Cd] complexes. This research offers a sustainable, cost-effective approach for Cd removal from industrial wastewater, addressing environmental pollution and agricultural waste management (Liu et al., 2022a). By converting agricultural residues into functional materials for pollutant removal, the study supports sustainable practices, optimizes resource utilization, reduces the demand for virgin materials, and promotes a circular economy, fostering long-term environmental and economic sustainability (Osman et al., 2024).

2. Materials and methods

2.1. Experimental framework

In this experiment, biochar was prepared from sawdust and then treated using various modification methods. The modified biochar was subsequently tested for its ability to adsorb the heavy metal Cd under different environmental conditions. This study aims to explore how different modification methods affect the properties of biochar and its Cd adsorption capabilities. The detailed modification steps are illustrated in (Scheme 1).

2.2. Preparation and sulfur modification of biochar

In this study, biochar was prepared from sawdust and modified to enhance its cadmium (Cd) adsorption capacity. Pristine biochar (SDB350) was produced by pyrolyzing sawdust at 350 °C for 4 h under oxygen-limited conditions with a nitrogen flow rate of 1.0 L min^{-1} (Shen et al., 2012; Chang et al., 2023). The resulting biochar, with a carbonization yield of 0.57–1.83%, was ground to ≤0.15 mm and washed until pH stabilization (Hwang et al., 2024).

Sulfur (S) modification of the pristine biochar involved both post-carbonization and pre-carbonization methods.

- ***Post-carbonization*** modification included immersion in sulfuric acid (H_2SO_4) solutions (96%) and 2.0 M sodium sulfide (Na_2S) at a 1:10 (w/v) ratio for 24 h (Yin et al., 2022b), separately.

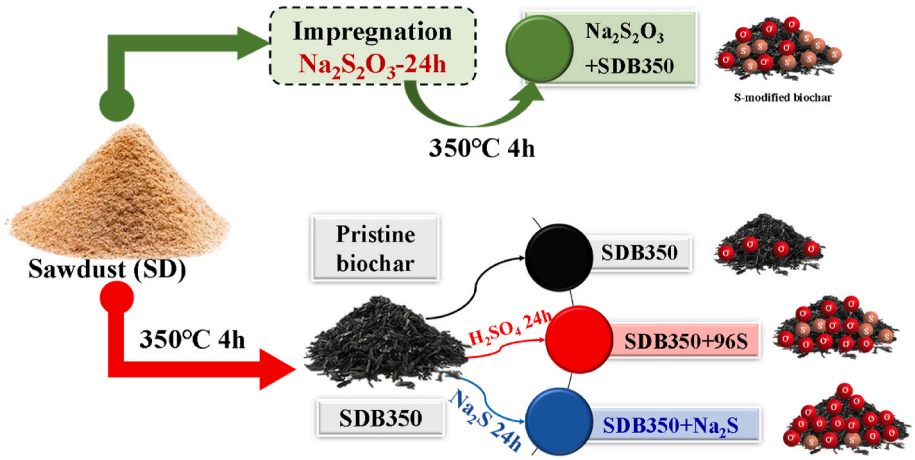

Scheme 1. Flowchart showing the preparation of pristine and S-modified sawdust biochars.

- ***Pre-carbonization*** modification involved treating raw sawdust with 2 M sodium thiosulfate ($Na_2S_2O_3$) solution before pyrolysis (Chen et al., 2024).

Our preliminary experiments evaluated various sulfur-containing modifiers: H_2SO_4 (10%, 30%), Na_2S, and $Na_2S_2O_3$ (0.5M, 2M), applied pre- and post-carbonization (**SI**). Four representative samples were selected based on performance, stability, and industrial scalability criteria, ensuring optimal modification outcomes for practical applications. As a result, ***four representative samples were selected for further study:***

- **SDB350**: Pristine biochar (sawdust carbonized at 350°C for 4 hours).
- **SDB350+96S**: SDB350 treated with 96% H_2SO_4 after carbonization.
- **SDB350+Na_2S**: SDB350 treated with 2M Na_2S after carbonization.
- **$Na_2S_2O_3$+SDB350**: SDB350 pre-treated with 2M $Na_2S_2O_3$ before carbonization.

The remaining samples were treated as preliminary results, and their Cd adsorption capacities are reported in the supporting information (**SI**).

2.3. The effect of pH on Cd adsorption

The effect of pH on Cd adsorption was investigated over a range of 2.0–9.0, using 0.04 g adsorbent in 40 mL of 0.01 M $NaNO_3$ solution with 50 mg L^{-1} Cd (Rajendran et al., 2022). The impact of biochar dosage was examined using 0.02, 0.04, and 0.08 g of adsorbent in 40 mL solution (0.5, 1, and 2 g L^{-1} ratios) with 50 mg L^{-1} initial Cd concentration. All experiments maintained a pH of 5.0 and a temperature of 25 °C, with samples filtered through 0.22 μm cellulose acetate membrane filters (MF-Millipore™) before ICP-OES analysis.

These comprehensive studies were designed to clarify the adsorption dynamics and assess the effectiveness of S-modified biochar for Cd removal from aqueous solutions, contributing to the development of sustainable and cost-effective remediation strategies. Detailed kinetic and isotherm models used to interpret the experimental data are provided in the Supporting Information (**SI**).

2.4. Spectroscopic analyses of biochar and Cd-loaded biochar

The elemental composition of pristine and S-modified biochar was quantified using an Elementar Vario EL cube-CHNOS analyzer. Nitrogen adsorption-desorption isotherms at 77K, essential for determining the BET surface area, pore surface area, and pore volume, were measured using a Quantachrome Instruments autoSorb iQ-TPX analyzer. The point of zero charge (pH_{pzc}) of biochar was measured by the pH shift method as proposed by (Lopez-Ramon et al., 1999). Morphological characteristics were analyzed with a ZEISS Ultra Plus Field Emission Scanning Electron Microscope (FE-SEM) equipped with energy-dispersive X-ray spectroscopy (EDS) for elemental analysis. Fourier transform infrared (FTIR) spectra of both untreated and Cd-loaded biochar were obtained using a Thermo Nicolet Nexus 6700 spectrometer. Additionally, X-ray photoelectron spectroscopy (XPS) analyses were conducted with a Thermo Scientific theta probe instrument to investigate elemental valence states and changes in the bonding energy resulting from Cd adsorption.

2.5. Simulation experiment

To explain the molecular-level interaction mechanism between cadmium (Cd) and both pristine and S-modified biochar, frontier molecular orbital calculations were conducted using Gaussian 16 at the B3LYP/LANL2DZ level of theory (Curtiss et al., 2007). The pristine biochar (SDB350) was modeled as a graphene-like sheet with epoxide, hydroxyl, and carboxyl functional groups, while the S-modified biochar incorporated two sulfur atoms doped into the graphene-like structure (Yu et al., 2024). Cd interaction was simulated by placing a Cd atom between graphene oxide sheets (for SDB350) and sulfur-doped graphene oxide sheets (for S-modified biochar) (Yang et al., 2022; Chen et al., 2018; de Carvalho et al., 2018; Elgengehi et al., 2020). The highest occupied molecular orbital (HOMO) and lowest unoccupied molecular orbital (LUMO) were analyzed, and band gaps were calculated before and after Cd interaction to assess electronic properties, charge transfer processes, and reactivity (Gariganti et al., 2024). This comprehensive analysis, including optimized structures and frontier molecular orbital analysis, provided insights into the reaction mechanism, electronic transitions, and the role of oxygen and sulfur doping in enhancing Cd adsorption capabilities, facilitating a deeper understanding of the reaction pathway and the relative affinity of Cd towards pristine and S-modified biochar (He et al., 2024; Vijayakumar et al., 2024; Yu et al., 2024).

3. Results and discussions

3.1. Elemental analysis

The elemental composition of pristine sawdust (SDB350) and its derived sulfur-modified biochar was analyzed (Table S1). In the pristine sawdust feedstock prior to carbonization, carbon (C), oxygen (O), and hydrogen (H) were the predominant elements, while nitrogen (N) and sulfur (S) were present in negligible quantities (0.00–0.09%). However, subsequent to the carbonization process, SDB350 exhibited a significant

enrichment in carbon content accompanied by a substantial decrease in oxygen (reduced by over 50%–23.29%) and hydrogen content compared to the pristine material. The relatively high residual oxygen content observed in SDB350, in comparison with other biochar materials derived from sources such as rice straw (Phuong and Loc, 2022), can be attributed to the higher lignin content in wood chips. The complete conversion of lignin to aromatic structures typically necessitates temperatures exceeding 400 °C.

The carbonization process facilitated the concentration of carbon by selectively removing volatile matter and non-carbonaceous elements, resulting in a carbon-enriched matrix. Simultaneously, the substantial reduction in oxygen and hydrogen content can be ascribed to the decomposition and volatilization of oxygen- and hydrogen-containing functional groups during the thermal treatment. The retention of a considerable fraction of oxygen in the SDB350 biochar can be explained by the recalcitrant nature of lignin, a major component of wood biomass, which requires higher temperatures for complete aromatization and deoxygenation (Fawzy et al., 2021).

Subsequent sulfur modification of the SDB350 biochar with concentrated H_2SO_4, 2M Na_2S, or 2M $Na_2S_2O_3$ resulted in a notable enhancement of sulfur content, with the extent of sulfur incorporation following the descending order: $Na_2S_2O_3$-modified SDB350 (12.96%) > SDB350 modified with 96S (2.81%) > Na_2S-modified SDB350 (0.43%) > pristine SDB350 (0.11%). Concomitantly, post-modification, SDB350 exhibited a significant augmentation in oxygen content, suggesting the introduction of oxygen-containing functional groups. The oxygen content followed an inverse trend: SDB350 modified with 96S (34.15%) > Na_2S-modified SDB350 (33.30%) > $Na_2S_2O_3$-modified SDB350 (29.12%) > pristine SDB350 (23.29%) (Table S1).

The modifications introduced sulfur and oxygen-containing functional groups onto the biochar surface, enhancing its adsorption capabilities for applications like heavy metal removal or catalysis. Notably, the substantial increases in sulfur and oxygen percentages could significantly boost cadmium adsorption. Sulfur heteroatoms facilitate functional group formation, which can effectively interact with cadmium ions through surface complexation, ion exchange, and Cd-O bond formation. Additionally, sulfur doping introduces more active sites and modifies the biochar's surface properties, further enhancing adsorption capacity.

Modification with sulfur compounds also decreased H/C and O/C ratios, indicating increased aromaticity while retaining oxygen functionalities. This shift from aliphatic to aromatic structures, along with enhanced sulfur and oxygen groups, improved hydrophilicity compared to pristine biochar, suggesting increased ion exchange and complexation capabilities. These modifications potentially enhance the cadmium removal performance of SDB350 biochar by promoting cadmium fixation through surface complexation, ion exchange, Cd-O bond formation, enhanced hydrophilicity, and additional active sites from sulfur doping (Leng et al., 2022).

3.2. BET surface area

The changes in specific surface area and pore volume of pristine and sulfur-modified biochar, before and after the sulfur modification process, are presented in (Fig. 1 a and Table S 2). Sulfur modification of SDB350 resulted in a significant increase in the specific surface area, rising from 4.85 $m^2\ g^{-1}$–8.26 $m^2\ g^{-1}$ with H_2SO_4, 10.70 $m^2\ g^{-1}$ with Na_2S, and a substantial 20.88 $m^2\ g^{-1}$ with $Na_2S_2O_3$. Concurrently, the pore volume of SDB350 expanded from 0.016 $cm^3\ g^{-1}$ to a range of 0.028–0.043 $cm^3\ g^{-1}$, accompanied by an increase in micropore volume from 0.002 $cm^3\ g^{-1}$ to 0.012–0.043 $cm^3\ g^{-1}$ across the three sulfur modification techniques. The modest increase in specific surface area, pore volume, and micropore volume after carbonization at 350 °C aligns with existing literature (Zhao et al., 2018), suggesting that more pronounced alterations typically occur at higher carbonization temperatures (>500–600 °C) (Ahmed et al., 2023; Mishra et al., 2023). Although the enhancements were relatively modest, they were potentially attributable to the introduced fragments or functional groups partially occupying and obstructing certain pores within the structure. Despite these minor increments in specific surface area and pore volume after sulfur modification, these changes may contribute additional adsorption sites and facilitate the mass transfer of adsorbate molecules, potentially playing a synergistic role in augmenting the Cd adsorption capabilities of the S-modified biochar (Petrovic et al., 2022; Ma et al., 2023).

3.3. pH and point of zero charge (pH_{pzc}) of biochar

The pH_{PZC} of the biochar samples, determined by the pH drift method, along with their respective pH values (biochar to water ratio of 1:20, w/w), are presented in (Table S 3). The pristine SDB350 biochar exhibited a pH of 4.61, attributable to the lower ash content in the pristine sawdust feedstock, which contains fewer alkali and alkaline earth metal oxides that impart basicity to the biochar. Following sulfur modification, a significant decrease in pH_{PZC} was observed, from 6.39 for the pristine SDB350 to 4.31 (H_2SO_4), 5.48 (Na_2S), and 4.60 ($Na_2S_2O_3$). This reduction in pH_{PZC} suggested that the S-modified biochar surfaces carried a higher density of negative charges at the same solution pH, facilitating electrostatic attraction and providing an

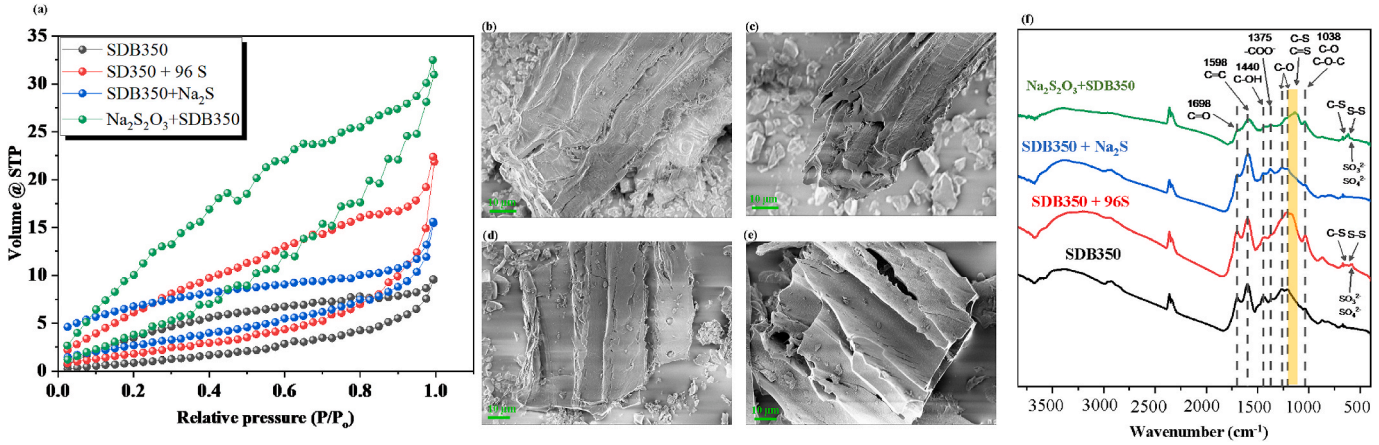

Fig. 1. Characterization of pristine and sulfur-modified sawdust biochar. (a) N_2 adsorption–desorption isotherms of pristine biochar (SDB350) and sulfur-modified biochars prepared using different methods: H_2SO_4 treatment (SDB350 + 96S), Na_2S impregnation (SDB350+Na_2S) (post pyrolysis), and $Na_2S_2O_3$ impregnation ($Na_2S_2O_3$+SDB350) (pre pyrolysis). (b–e) Scanning electron microscopy (SEM) images of: (b) SDB350; (c) SDB350 + 96S; (d) SDB350+Na_2S; (e) $Na_2S_2O_3$+SDB350. (f) Fourier-transform infrared (FTIR) spectra of pristine and S-modified sawdust biochars.

increased number of active sites for the adsorption of positively charged Cd ions. The enhanced negative surface charge and the presence of oxygen and sulfur-containing functional groups were expected to synergistically augment Cd adsorption onto the S-modified biochar, a phenomenon corroborated by adsorption experiments (Ma et al., 2024). Further detailed information about pHpzc characterization and its significance can be found in the Supporting Information (**SI**).

3.4. SEM and EDS analyses of pristine and S-modified biochar

Scanning electron microscopy (SEM) imaging and energy-dispersive X-ray spectroscopy (EDS) analyses were conducted to investigate the surface morphology and elemental composition of pristine and sulfur-modified sawdust biochar samples (Table S 4). The SEM micrographs showed a relatively smooth surface morphology for the pristine SDB350 biochar, which transformed into conspicuously rougher textures adorned with wrinkles, cracks, and pores upon the sulfur-modification processes (Fig. 1 b ~ e). Notably, SEM images showed a more expanded, exfoliated and porous texture with increased surface area for the $Na_2S_2O_3$+SDB350 sample (Ahmed et al., 2021), suggesting a uniform influence of the sulfur-modification treatments on the surface morphology, corroborating the findings from the BET analyses.

EDS results showed a significantly higher oxygen (O) content on the pristine SDB350 surface compared to the bulk elemental analysis (Table S 4), indicating the enrichment of oxygen-containing functional groups on the surface. After sulfur modification, the EDS O content increased, though not as substantially as the bulk elemental analysis, suggesting that some newly introduced oxygen-containing functional groups were incorporated within the internal biochar structures. Similarly, the EDS sulfur (S) contents were generally higher than those obtained from elemental analyses (Table S 1), implying that a significant fraction of the sulfur moieties was concentrated on the biochar surface.

Notably, the EDS analysis presented the highest oxygen (O) content in the SDB350 + 96S biochar among other biochars and sulfur-modified biochars, corroborating the elemental analysis results. Moreover, the $Na_2S_2O_3$+SDB350 sample exhibited a lower O content than the pristine SDB350, likely due to a substantial increase in surface sulfur (S) concentration or the incorporation of sulfur-containing functional groups through esterification reactions. The increased S and O content obtained via the EDS analysis strengthens the evidence of successful sulfur and oxygen functionalization, supporting the elemental analysis findings. These surface modifications could play a crucial role in enhancing cadmium adsorption by facilitating the anchoring of cadmium ions through interactions with oxygen functional groups, further aided by the presence of sulfur moieties on the biochar surface (de Falco et al., 2018).

3.5. FTIR analysis of pristine and S-modified biochar

Multiple absorption peaks were observed within the wavenumber range of 1200–1700 cm^{-1}, attributed to C=O, C=C, -COO-, and C-O stretching on the SDB350 biochar (Fig. 1f–Table S 5). Upon modification with S-containing compounds, enhanced signals at 563-617 cm^{-1} (SO_4^{2-}), 600-620 cm^{-1} (SO_3^{2-}), 630-660 cm^{-1} (S-S), and 1100-1200 cm^{-1} (C-S, C-S with C=S) indicated an increase in sulfur functional groups, particularly for $Na_2S_2O_3$+SDB350 sample, suggesting a more pronounced integration of sulfur-containing functional groups into the biochar. Additionally, increased peaks at 1038 cm^{-1} (C-O, C-O-C) and 1200-1275 cm^{-1} (C-O in aryl ethers) and at 1375 cm^{-1} (-COO-) and 1698 cm^{-1} (C=O) indicated the formation of more O-containing groups, carboxyl, and ester groups during modification with S-containing compounds, corroborating the introduction of both oxygen and sulfur functionalities on SDB350. SDB350 + 96S exhibited a significant increase in the 3200-3400 cm^{-1} range (O-H stretch), likely resulting from the higher lignin content in sawdust biochar, which led to lower aromatization at 350 °C, facilitating functionalization during modification (He et al., 2021). Furthermore, the oxygen functionalities introduced through the modification process are anticipated to contribute synergistically with the sulfur modifications, significantly enhancing cadmium adsorption. These oxygen moieties are expected to facilitate the formation of strong cadmium-oxygen complexes, while the sulfur enrichment is likely to enhance the electronic configurations, thereby promoting favorable Lewis acid-base interactions between the biochar surface and cadmium ions. The synergistic effects arising from the interplay of these surface modifications, facilitating cadmium immobilization through multiple mechanisms, will be illuminated in greater detail in subsequent discussions.

3.6. XPS analysis of biochar

The surface composition changes during modification were analyzed via XPS, focusing on C 1s, O 1s, and S 2p spectra of sawdust biochar (SDB350) before and after treatment (Fig. 2, Fig. S 2~S 5; Table S 6). In the C 1s spectrum, the vanishing of the C=O signal and the emergence of O-C=O following sulfur modification paralleled observations made in other crop residue biochar (Wan et al., 2022). The O 1s spectrum showed a shift from C-O-C/C-O dominance in pristine SDB350 to increased C=O and COOH content post-sulfur modification, with a new S-O signal following $Na_2S_2O_3$ treatment.

Initially, no sulfur signal was detected in the S 2p spectrum of SDB350 biochar, but weak signals emerged at 164.2 and 169.0 eV after Na_2S modification. A significant increase was observed after H_2SO_4 and $Na_2S_2O_3$ treatments, consistent with the results of elemental analysis and FTIR. Notably, the $Na_2S_2O_3$+SDB350 sample exhibited double-peak S 2p signals, indicating differing functional groups compared to those seen with H_2SO_4-treatment SDB350. Peaks at 168.1–169.2 eV and 169.1–170.2 eV, corresponding to -SO_3^{2-} and -SO_4^{2-}, respectively, were observed with H_2SO_4 treatment. Conversely, $Na_2S_2O_3$ treatment exhibited peaks at 163.7–163.9 eV and 164.8–165.1 eV, suggesting the presence of S^{2-}, C-S, C=S, S-S, and -SH, as corroborated by the FTIR results. Consistent with FTIR spectra (Fig. 1 f), -SO_3^{2-} signals appeared for both H_2SO_4 and $Na_2S_2O_3$ treatments; however, only $Na_2S_2O_3$ exhibited notable enhancements in C-S, C=S, and S-S. Sulfur treatments on carbon materials introduce oxygen and sulfur functional groups on the surface. These groups are expected to facilitate cadmium adsorption through oxygen-cadmium bonding, enhanced by the enriched electronic configuration from sulfur doping. Consequently, the oxygen-sulfur-treated carbons could exhibit improved adsorption and reactivity toward organic and inorganic pollutants (Petrovic et al., 2022).

3.7. Adsorption kinetics of Cd on biochar

Pristine SDB350 exhibited relatively slower adsorption kinetics, attaining equilibrium at 360 and 240 min for initial Cd concentrations of 5 and 40 mg L^{-1}, respectively (Fig. 3, Fig. S 6). In contrast, sulfur-modified biochars demonstrated significantly accelerated adsorption kinetics. Notably, SDB350 + 96S reached equilibrium within 5 min for both 40 and 150 mg L^{-1} initial concentrations, while $Na_2S_2O_3$+SDB350 displayed the most rapid kinetics, achieving equilibrium within 5 min across all initial Cd concentrations examined. These remarkable enhancements in adsorption kinetics by sulfur modifications underscore their effectiveness in enabling near-instantaneous Cd removal from aqueous solutions.

The adsorption mechanism was investigated by carefully fitting kinetic adsorption equilibrium data to both pseudo-first-order and pseudo-second-order kinetic models. This analysis aimed to shed light on the underlying adsorption process. The fitting results (Fig. 3, Fig. S 6, Table 1) unambiguously revealed that the coefficient of determination (R^2) values for the pseudo-second-order model were consistently ≈0.999, indicating its superior fit for the kinetic adsorption data compared to the pseudo-first-order model. Furthermore, the experimental equilibrium adsorption capacities (q_t) at an initial Cd concentration of 40 mg L^{-1} closely aligned with the theoretical values (q_e)

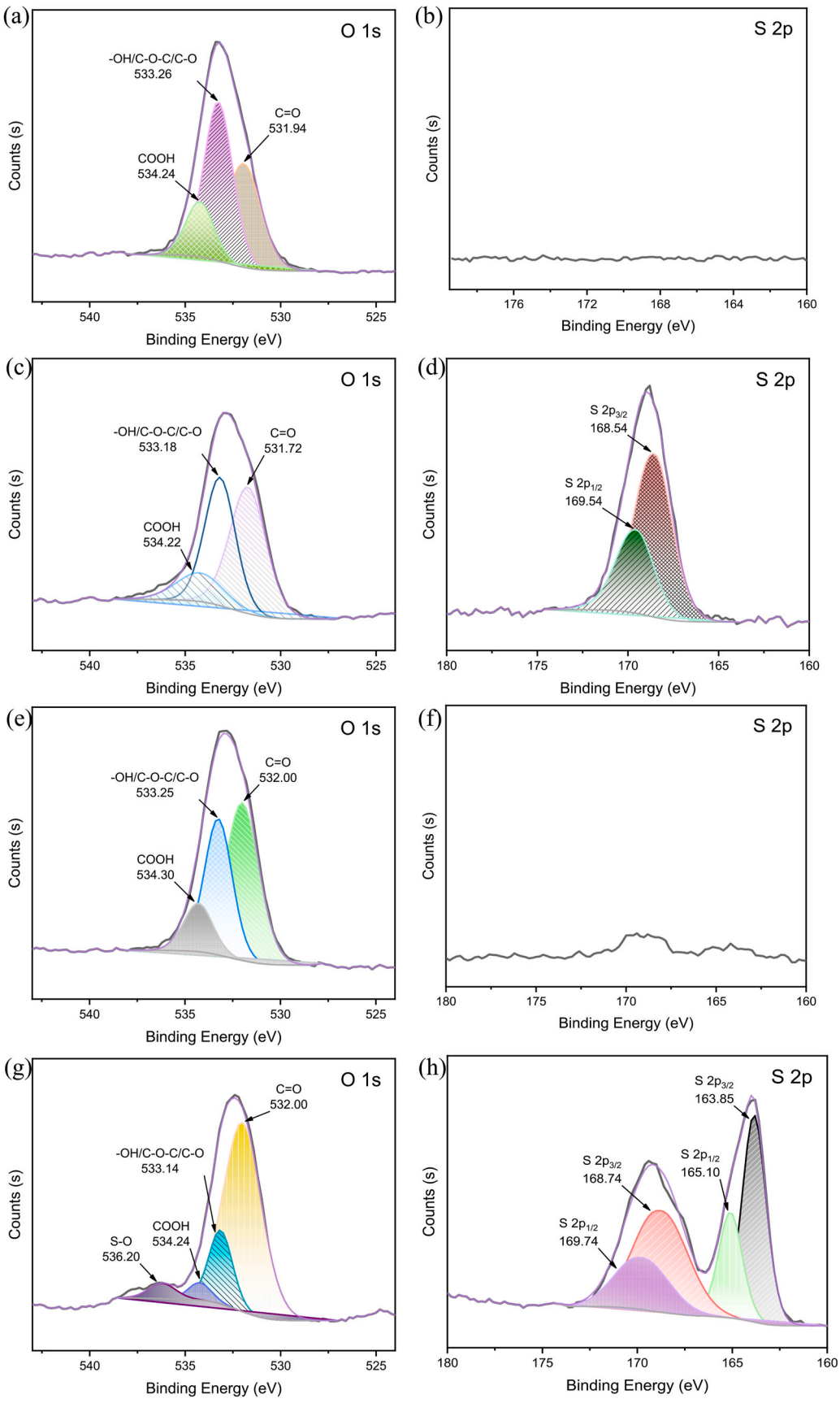

Fig. 2. XPS S 2p and O 1s spectra for (a,b) pristine SDB350; (c,d) SDB350 with 96 % H_2SO_4 (SDB350 + 96S); (e,f) SDB350 treated with Na_2S (SDB350+Na_2S); (g,h) SDB350 pre-treated with $Na_2S_2O_3$ ($Na_2S_2O_3$+SDB350).

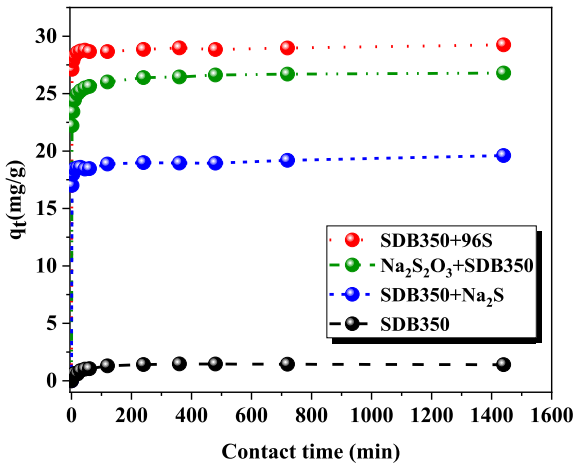

Fig. 3. Cadmium adsorption kinetics by pristine and S-modified sawdust biochars (SDB350, SDB350 + 96S, SDB350+Na_2S, $Na_2S_2O_3$+SDB350) at initial Cd^{2+} 40 mg L^{-1}, adsorbent 1.0 g L^{-1}, pH 5.0 in 0.01 M $NaNO_3$. Data points: experimental Cd concentrations; solid lines: pseudo-second-order kinetic model fits.

Table 1
The kinetic adsorption parameters of Cd by pristine and S-modified sawdust biochar at pH 5.0.

Kinetic Models	Pseudo first order			Pseudo second order		
	k_1 (min^{-1})	q_e	R^2	k_2 (g mg^{-1} min^{-1})	q_e	R^2
SDB350	0.002	0.437	0.432	0.062	1.430	0.999
SDB350 + 96S	0.002	0.837	0.511	0.021	29.203	0.999
SDB350+Na_2S	0.002	1.299	0.666	0.012	19.533	0.999
$Na_2S_2O_3$+SDB350	0.005	2.102	0.898	0.017	26.804	0.999

k_1 (min^{-1}) and k_2 (g mg^{-1} min^{-1}) represent the rate constants for the pseudo-first-order and pseudo-second-order kinetic models, respectively. (q_e) represents the equilibrium adsorption capacity of the adsorbent.

predicted by the pseudo-second-order kinetic model, further corroborating its applicability.

The unequivocal superiority of the pseudo-second-order kinetic model strongly suggests that the adsorption rate was predominantly governed by chemisorption processes, such as surface complexation. The absence of a slow adsorption transition phase before saturation indicated that the abundant functional groups introduced on the modified biochar surfaces provided numerous active sites for rapid adsorption, predominantly occurring on the external surfaces.

Notably, the markedly higher kinetic adsorption parameter observed for S-modified biochars compared to pristine biochar accentuates the remarkable efficiency of S and O functionalization in augmenting the adsorption kinetics for Cd removal. This observation underscores the pivotal role of surface functionalization in not only enhancing the adsorption quantities but also significantly improving the adsorption kinetics.

The consistent agreement between the experimental data and the pseudo-second-order kinetic model, coupled with the observed profound effects of surface functionalization, provides a coherent and robust understanding of the adsorption mechanism. The adsorption process is primarily governed by chemisorption interactions facilitated by the introduced functional groups, leading to rapid adsorption kinetics and substantial enhancements in adsorption capacities, particularly for the S-modified biochars (Rafiq et al., 2023).

3.8. Isotherm adsorption patterns of biochar

The adsorption of cadmium (Cd) onto pristine and S-modified sawdust biochar was systematically investigated under controlled conditions: a pH of 5.0, a temperature of 25 °C, an adsorbent dosage of 1 g L^{-1}, and an adsorption time of 24 h. Initial Cd concentrations ranged from 5 to 200 mg L^{-1}. The adsorption process exhibited a rapid increase at lower concentrations, followed by a gradual approach to equilibrium, suggesting a high affinity of biochar for Cd at low concentrations, which stabilizes as the adsorption sites become saturated.

To explain the relationship between Cd accumulation on the biochar surface and the concentration of Cd in solution, the equilibrium adsorption data were fitted to the Langmuir and Freundlich adsorption models (Fig. 4, Table 2). The Langmuir model, which assumes monolayer adsorption on a homogeneous surface with no interactions between adsorbed ions, provided a better fit for the data, as indicated by higher correlation coefficients (R^2). This suggests that the adsorption of Cd onto both pristine and S-modified biochar occurs primarily as a monolayer on a uniform surface. The maximum adsorption capacities (q_m) derived from the Langmuir model for various biochar samples are as follows: SDB350 + 96S: 39.38 mg g^{-1}, $Na_2S_2O_3$+SDB350: 34.14 mg g^{-1}, SDB350+Na_2S: 20.84 mg g^{-1}, and SDB350: 4.37 mg g^{-1}. The pristine sawdust biochar modified with 96% H_2SO_4 (SDB350 + 96S) exhibited the highest adsorption capacity, approximately nine times greater than the pristine biochar.

The superior performance of SDB350 + 96S is attributed to its high oxygen content (34.15%), as determined by elemental analysis (Table S1). Despite having a lower sulfur content (2.81%) compared to $Na_2S_2O_3$+SDB350 (12.96% sulfur, 29.12% oxygen), the higher oxygen percentage appears to play a more crucial role in Cd adsorption. This indicates that oxygen-and sulfur-containing functional groups significantly enhance Cd adsorption, likely through enhanced Lewis acid-base interactions and electronic configurations.

Within the Cd concentration range of 0–200 mg L^{-1}, S-modified biochars consistently demonstrated higher adsorption capacities for Cd compared to the pristine biochar. The modifications introduced oxygen- and sulfur-containing functional groups, which were shown to play critical roles in the adsorption process. FTIR and XPS spectral analyses supported these findings, showing that biochar samples with higher concentrations of these functional groups exhibited superior adsorption capacities for Cd.

These findings highlight the importance of surface functionalization in enhancing biochar's adsorption performance. Specifically, introducing oxygen- and sulfur-containing groups through chemical modifications significantly improves Cd adsorption. Among the tested samples, biochar modified with 96% H_2SO_4 (SDB350 + 96S) exhibited the highest adsorption capacity, underscoring the critical role of oxygen content. These insights are valuable for designing and applying modified biochar for effective heavy metal remediation (Zhou et al., 2020).

3.9. Effects of pH on Cd removal by biochar

The effect of initial pH on Cd removal by pristine and S-modified sawdust biochar was investigated under the following conditions: 0.01 M $NaNO_3$ background solution, a solid-liquid ratio of 1 g L^{-1}, and an initial Cd concentration of 50 mg L^{-1}. Cadmium removal efficiency showed an increasing trend with rising pH (Fig. S 7). At a pH of 2, pristine SDB350 exhibited a removal efficiency of only 0.86%, which improved significantly after modification: 24.75% with H_2SO_4, 3.11% with Na_2S, and 23.13% with $Na_2S_2O_3$, respectively. As the pH increased to 9, the removal efficiencies soared to 79.44% for SDB350, 99.36% for SDB350 + 96S, 99.60% for SDB350+Na_2S, and 97.72% for $Na_2S_2O_3$+SDB350. However, MINTEQ calculations (Fig. S 8) indicated potential Cd precipitation at pH levels of 7–8, suggesting the high removal efficiencies observed above pH 7 were likely due to precipitation rather than biochar adsorption. Notably, in the pH range of 4–7,

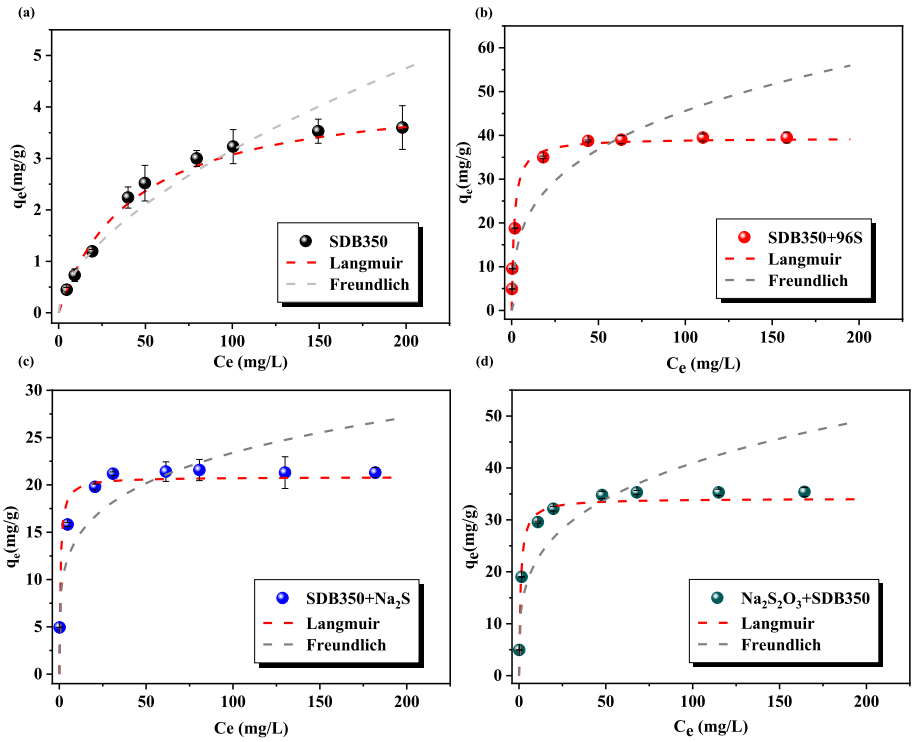

Fig. 4. Cadmium adsorption isotherms for pristine and S-modified sawdust biochars at 1.0 g L^{-1} dosage, pH 5.0, 24 h contact time. Initial Cd concentrations: 5, 40, 150 mg L^{-1}. Circles represent experimental data; dashed lines show Langmuir/Freundlich model fits: (a) SDB350; (b) SDB350 + 96S; (c) SDB350+Na_2S; (d) $Na_2S_2O_3$+SDB350.

Table 2
The isotherm adsorption parameters of Cd by pristine and S-modified sawdust biochar at pH 5.0.

Isothermal Models	Langmuir			Freundlich		
	K_L	q_m (mg g^{-1})	R^2	K_F	1/n	R^2
SDB350	0.02	4.37	0.991	0.21	0.59	0.944
SDB350 + 96S	0.67	39.38	0.994	11.27	0.30	0.927
SDB350+Na_2S	1.57	20.84	0.995	8.73	0.21	0.876
$Na_2S_2O_3$+SDB350	1.03	34.14	0.998	11.92	0.27	0.855

K_L and K_F are the equilibrium adsorption constants for the Langmuir and Freundlich adsorption models, respectively. (q_m) is the maximum adsorption capacity of the adsorbent (mg g^{-1}), and 1/n is an empirical constant representing the adsorption intensity of the system.

where adsorption is the predominant mechanism, the removal efficiency for most biochar showed a gradual increase from pH 4 to 6, followed by a sudden rise between pH 6 to 7.

The SDB350+Na_2S sample showed significantly lower removal efficiencies than other sulfur-modified biochar below pH 6, attributable to its higher pH_{pzc} value, which necessitated a higher pH to develop negative surface charges. At pH 5.0, the Cd removal performance mirrored the pH_{pzc} values, with the sequence being 96S > $Na_2S_2O_3$ > Na_2S > pristine SDB350. This confirmed that biochar with lower pH_{pzc} values and higher negative surface charges demonstrated stronger attraction towards Cd ions, resulting in enhanced adsorption. Based on these observations, pH 5.0 was selected as the optimal initial pH condition for subsequent adsorption experiments, aligning with previous studies that identified the pH range of 5–6 as optimal for Cd adsorption by biochar (Xia et al., 2023).

3.10. Effect of different biochar dosages on Cd removal

Under the conditions of 0.01 M $NaNO_3$ background solution, a pH of 5.0, and an initial Cd concentration of 50 mg L^{-1}, the impact of varying biochar dosages (0.5, 1.0, and 2.0 g L^{-1}) on Cd adsorption capacity and removal efficiency was investigated. The changes in the Cd adsorption capacity of pristine and S-modified sawdust biochar at different dosages are depicted in (Fig. 5 a). Most biochar exhibited maximum adsorption capacities at a dosage of 1.0 g L^{-1}, while the capacities were lowest at 2.0 g L^{-1}. Although the removal efficiency was highest at 2.0 g L^{-1} (Fig. 5 b), many adsorption sites remained unutilized. This indicated that a dosage of 1.0 g L^{-1} provided better utilization of adsorption sites, making it more efficient and economical. Based on these observations, a biochar dosage of 1.0 g L^{-1} was selected as the optimal condition for subsequent experiments. This dosage provided a balance between effective utilization of adsorption capacity and high removal efficiency.

3.11. Adsorption mechanism

3.11.1. The role of C and O on biochar

Fourier-transform infrared (FTIR) spectroscopy was employed to illustrate the role of functional groups on biochar in the Cd adsorption process (Fig. S 9). depicts the FTIR spectra of pristine biochar (black line) and Cd-loaded biochar (red line) after the adsorption process. A noticeable shift in the C=C stretching vibration (1594-1600 cm^{-1}), associated with aromatic structures, was observed for pristine sawdust biochar and S-modified sawdust biochar upon Cd adsorption. This shift indicates interactions between the π electrons of aromatic structures and Cd ions (π-Cd^{2+}), suggesting their involvement in the adsorption mechanism (Wang et al., 2024). Signals corresponding to oxygen-containing functional groups, including C=O (1698 cm^{-1}), C-OH (1440 cm^{-1}), and -COO^- (1375 cm^{-1}), exhibited shifts after Cd adsorption. These shifts suggest the involvement of these groups in the adsorption process, which will be corroborated by computational

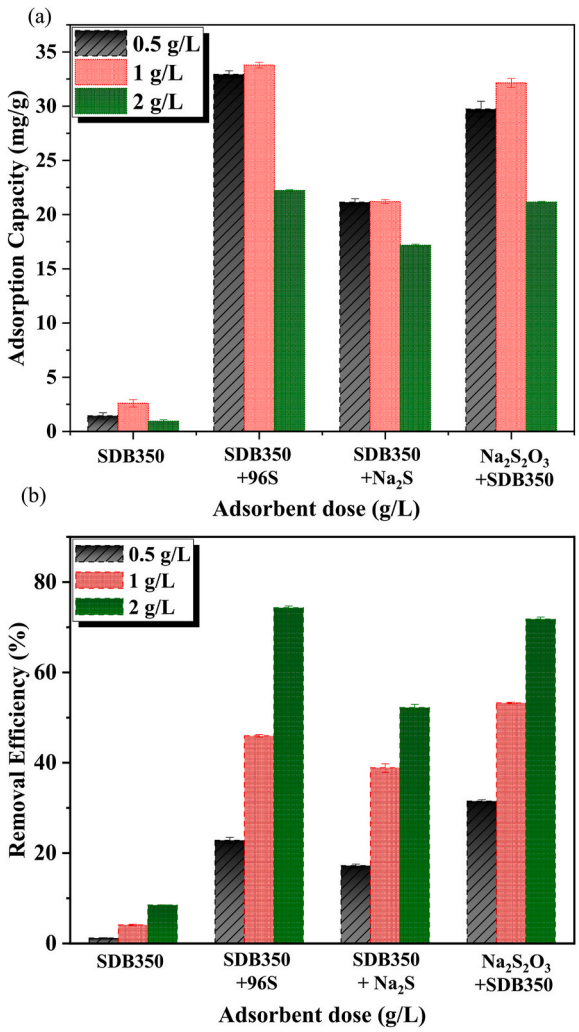

Fig. 5. Impact of pristine and sulfur-modified biochar dosages on cadmium (Cd) adsorption. (a) Adsorption capacity (mg g^{-1}) and (b) removal efficiency (%) of Cd^{2+} ions by pristine and S-modified sawdust biochar. Experimental conditions: initial Cd^{2+} concentration = 50 mg L^{-1}, pH 5.0, contact time = 24 h, temperature = 25 °C.

analysis later in this study. Previous studies have demonstrated that Cd can be adsorbed onto solid surfaces through surface complexation or surface precipitation mechanisms, as depicted in the following equations (1) and (2) (Li et al., 2024; Narmadha and Sreemahadevan, 2024).

X-ray photoelectron spectroscopy (XPS) analysis was conducted to investigate the surface chemistry and elemental composition of pristine and sulfur-modified sawdust biochar before and after Cd adsorption. The presence of Cd $3d_{3/2}$ and Cd $3d_{5/2}$ signals in the Cd 3d spectra after adsorption (Fig. 6, Fig. S 10~S 17) unambiguously confirms the successful adsorption of Cd onto the biochar surfaces. The C 1s spectra exhibited shifts in the binding energies of C-C/C=C (284.7 eV) and C=O (287.8 eV) after Cd adsorption, corroborating the FTIR analysis observations (Fig. S 9). These shifts suggest the involvement of π electrons from aromatic structures and carbonyl groups in the interaction with Cd ions (π-Cd^{2+}), contributing to the adsorption process. Moreover, the C 1s spectra revealed an increase in intensity and a shift in the binding energy of C-O (286.0–286.1 eV) after Cd adsorption.

For S-modified biochar, a notable increase in the O-C=O component proportion was observed in the C 1s spectra after Cd adsorption, accompanied by a significant decrease in the C=O component proportion in the O 1s spectra. These observations confirm the involvement of carbonyl, carboxyl, and ester groups in the adsorption process through ion exchange and complexation mechanisms (Scheme 2). In these processes, Cd ions are immobilized on functional groups (particularly carboxyl groups) on the biochar surface, leading to an increase in carboxylate salts. This will be further corroborated by computational analysis (Yin et al., 2022a). This phenomenon is consistent with the FTIR analysis results, which showed a decrease in the intensities of carboxyl-related signals and an increase in the carboxylate salt (-COO-) signal after Cd adsorption (Fig. S 9). The adsorption of Cd onto biochar can also be illustrated through the analysis of the C 1s and O 1s spectra obtained from XPS (Fig. 6, Fig. S 10~S 17). The presence of various components, such as C-C/C=C, C-O, O-C=O, and C=O in the C 1s spectra, and C=O, C-O-C/C-O, and COOH/OH in the O 1s spectra, suggests that the adsorption primarily occurs through electrostatic attraction between the π-electrons of aromatic structures and Cd ions, as well as through complexation with the oxygen and sulfur-containing functional groups present on the biochar surface (Scheme 2).

3.11.2. *The role of S on biochar*

The elemental analysis results (Table S1) displayed that the sulfur content of the biochar samples followed the order: $Na_2S_2O_3$+SDB350 > SDB350 + 96S > SDB350+Na_2S > SDB350, which correlated with the trend observed in the intensities of sulfur-related peaks in the FTIR

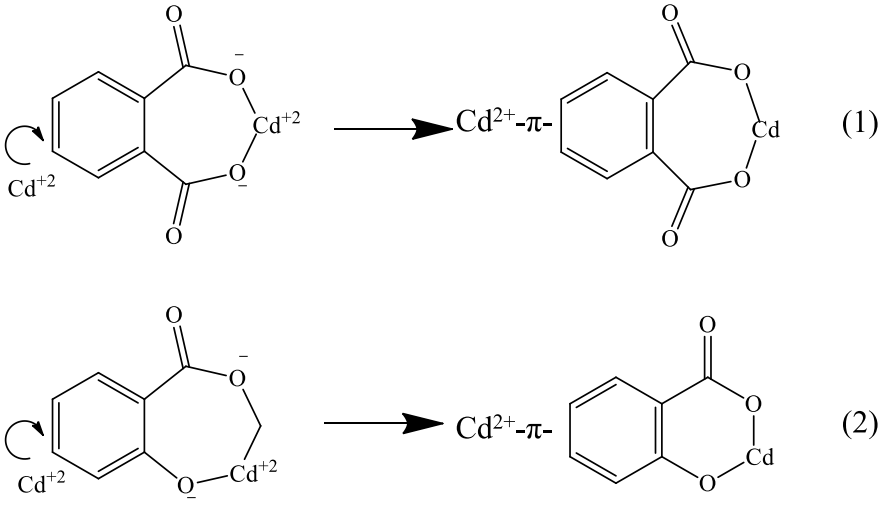

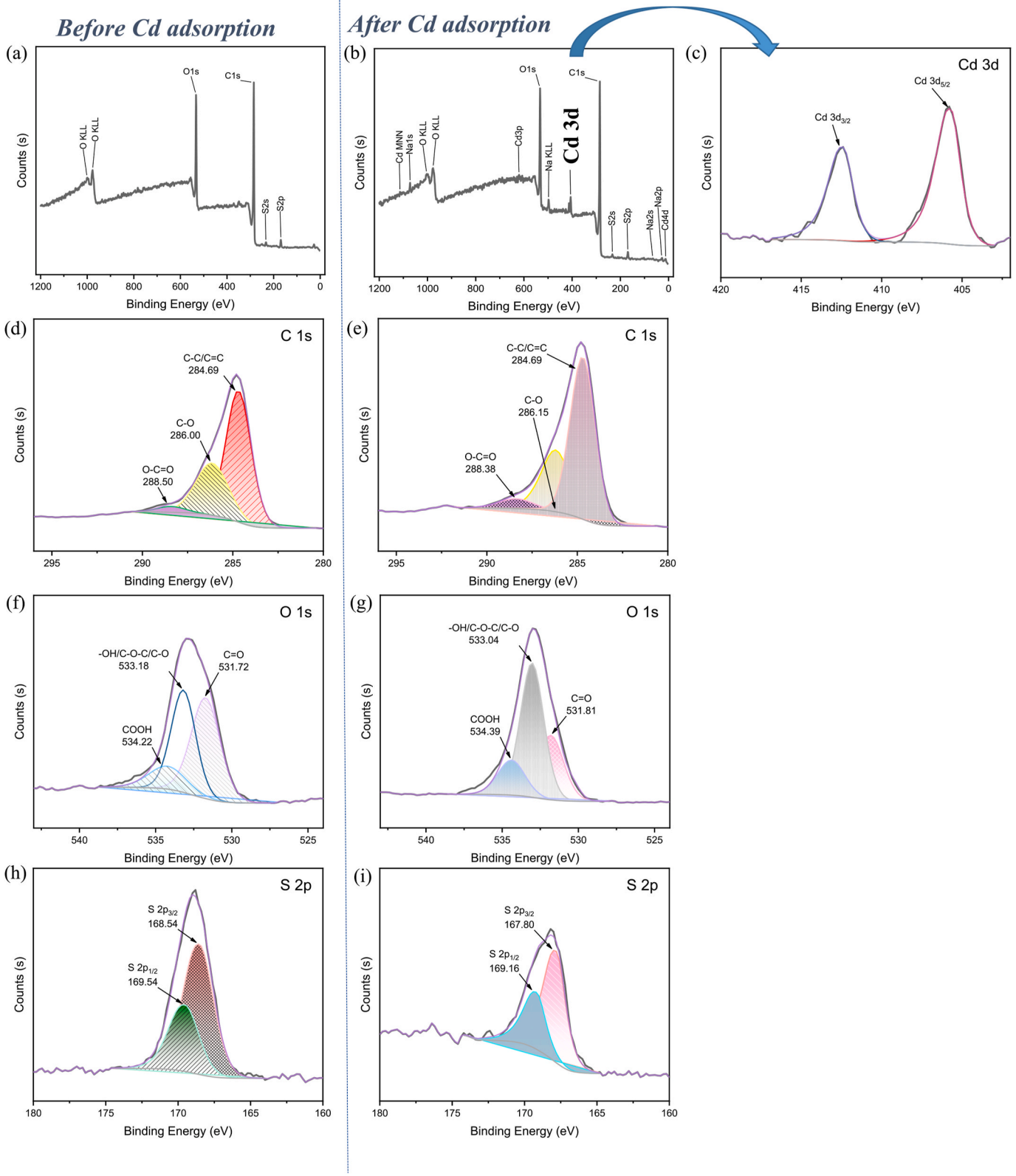

Fig. 6. XPS spectra of SDB350 + 96S before and after cadmium adsorption [(a, d, f, h) before adsorption]; [(b, e, g, i) after adsorption], [(c) Cd 3d].

spectra. These sulfur-containing functional groups ($SO4^{2-}$, $SO3^{2-}$, C-S, S-S, and C=S) exhibited shifts and decreases in intensity after Cd adsorption, suggesting their involvement in the adsorption process (Yin et al., 2022b). The S 2p spectra obtained from XPS corroborated the FTIR (Fig. S 9) and elemental analysis findings (Table S1), with more prominent S 2p signals observed for biochar treated with higher sulfur content (sodium thiosulfate modifications).

The incorporation of sulfur-containing functional groups through

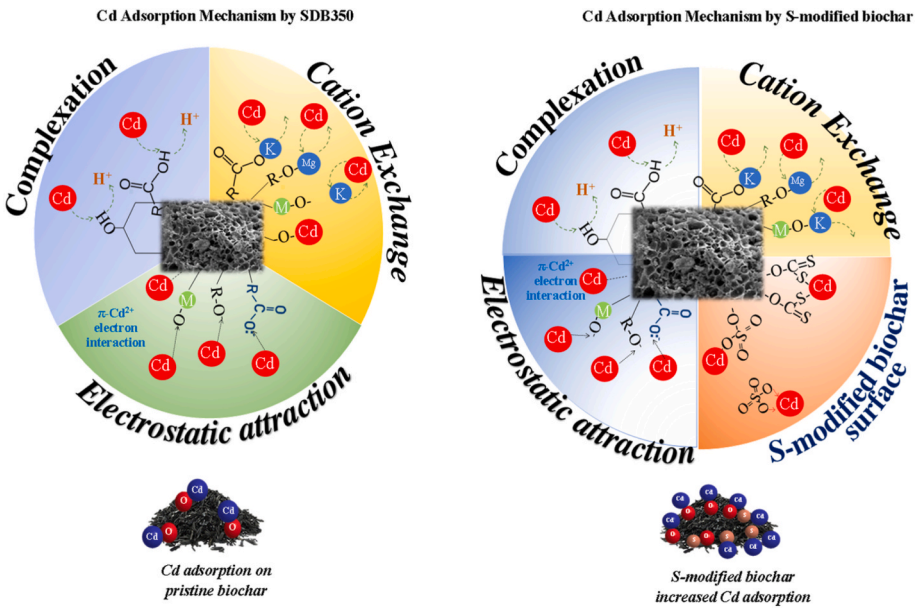

Scheme 2. Proposed mechanisms of cadmium adsorption by pristine and sulfur-modified biochars.

modifications significantly enhanced the adsorption capacity and selectivity towards Cd due to the higher affinity of these soft base functional groups towards the soft acid Cd ion, as predicted by Pearson's Hard and Soft Acids and Bases (HSAB) theory (Pearson and Songstad, 1967; Ho, 1975). The SEM-EDS elemental distribution results (Fig. S 18) further confirmed the enhanced affinity between the sulfur-containing functional groups and Cd ions in solution, as the distribution of adsorbed Cd on the biochar surface was more similar to that of sulfur.

According to Pearson's Hard and Soft Acids and Bases (HSAB) theory, soft acids (electron acceptors) tend to form stronger bonds with soft bases (electron donors) (Table S 7). Cadmium (Cd) is classified as a soft Lewis acid, while various sulfur-containing functional groups are considered soft Lewis bases. Consequently, the sulfur-containing functional groups on S-modified biochar exhibit a stronger affinity towards Cd.

Interestingly, Cd can also interact with oxygen-containing functional groups, which act as hard Lewis bases. This dual interaction potential suggests that Cd has an affinity for both oxygen- and sulfur-modified biochar. As a result, despite the reduction in carboxyl group content during the sulfurization process, the overall adsorption performance was enhanced. This improvement confirms the significant contribution of oxygen and sulfur-containing functional groups in boosting Cd adsorption onto biochar (Zhang et al., 2022; Chen et al., 2020a) reported an extreme case where organic compounds on the biochar surface gradually decomposed, consuming oxygen and reducing sulfate/sulfite groups to sulfides, which reacted with Cd oxides to form metal sulfides, resulting in Cd removal. The proposed reaction mechanisms involving sulfur-containing functional groups are illustrated in (Scheme 2) (Zhang et al., 2023a, 2023b).

3.11.3. The role of S and O on biochar

Furthermore, the oxygen content and percentage are expected to play an essential role in Cd adsorption through the formation of Cd-O bonds, as shown by the subsequent Density Functional Theory (DFT) calculations and simulations. The mechanism involves direct bonding between Cd and oxygen, which enhances Cd adsorption. Moreover, sulfur doping also enhances Cd adsorption through a synergistic effect. Therefore, it is necessary to maximize both oxygen and sulfur contents to achieve optimal Cd adsorption. This study clarifies the mechanism by which both sulfur and oxygen are necessary elements to enhance the synergistic effect of Cd adsorption. While a high sulfur content is beneficial, a sufficient amount of oxygen is also crucial. If only sulfur is high but the oxygen content is low, the Cd adsorption capacity is reduced, as observed for $Na_2S_2O_3$+SDB350 (34 mg g^{-1}) compared to SDB350 + 96S (39.38 mg g^{-1}) with higher oxygen content (34.15%) and lower sulfur content (2.81%). However, when the sulfur percentage increased to 12.96% while the oxygen amount decreased to 29.12%, the Cd adsorption capacity slightly decreased to 34.14 mg g^{-1} for $Na_2S_2O_3$+SDB350. This emphasizes the role of both sulfur and oxygen in enhancing Cd adsorption due to the formation of Cd-O bonds, which is further facilitated by the presence of sulfur in the compound, as supported by the DFT calculations. Correspondingly, when the sulfur amount was decreased to 0.43%, and the oxygen content was increased to 33.3% in SDB350+Na_2S, the Cd adsorption capacity reached 20.84 mg g^{-1}, which is lower due to the reduced sulfur content. Therefore, it is mandatory to increase both oxygen and sulfur contents to achieve higher Cd adsorption capacities. This is the first study to clarify the synergistic role of both oxygen and sulfur in enhancing Cd adsorption, investigated through practical and theoretical observations using DFT, as discussed in the subsequent sections.

3.11.4. Comparison with other sulfur modification studies

A comparison with related studies (Table 3) highlights the effectiveness of the sulfur modification methods employed, including sodium thiosulfate, sulfuric acid, and sodium sulfide treatments. While most reported sulfur modifications involve complex agents and multiple steps, with a maximum 6.75-fold increase in adsorption capacity, the simple sodium thiosulfate modification remarkably increased the sulfur content by 12.96% in sawdust biochar ($Na_2S_2O_3$+SDB350), enhancing the maximum Cd adsorption capacity by 9-fold (q_m = 34.14 mg g^{-1}) compared to pristine SDB350 (qm = 4.37 mg g^{-1}). Moreover, SDB350 + 96S, with 2.81% sulfur and 34.15% oxygen, exhibited the highest Cd adsorption of 39.38 mg g^{-1} among sawdust biochars. These substantial improvements through straightforward single-step processes demonstrate the simplicity and efficacy of sodium thiosulfate, sulfuric acid, and sodium sulfide modifications compared to complex reported methods.

These facile and cost-effective approaches exceptionally improve biochar's Cd adsorption performance. While previous studies employed intricate multi-step modifications with modest enhancements, this work showcases remarkable increases in Cd adsorption through simple sodium thiosulfate, sulfuric acid, or sodium sulfide treatments, contributing to efficient cadmium removal adsorbent development.

Table 3
Various heavy metals adsorption capacity of biochars before and after modification.

Modifier	Feedstock	T (°C)	Heavy metal	C_i (mg/L^1)	Dosage (g L^{-1})	Capacity (mg g^{-1})		Reference
						Before	After	
Thiourea	poplar	600	Cd	500	5.0	5.9	9.6	Zhu et al. (2020b)
Carbon disulphide	wheat straw	400	Cd	100	1.0	33.4	41.4	Chen et al. (2020a)
Iron nitrate ammonium tetrathiomolybdate	corn straw	600	Cd	300	1.0	17.8	68.8	Khan et al. (2020)
NaOH	rice husk	450	Cd	100	1.0	7.1	47.9	Chen et al. (2019)
Glutaraldehyde cystamine								
β-mercaptoethanol acetic anhydride	rice straw	500	Cd	600	2.5	14.2	45.1	Fan et al. (2020)
sulfuric acid			Pb			67.4	61.4	
Elemental sulfur	rice husk	550	Hg	200	2.0	38.8	67.1	O'Connor et al. (2018)
Elemental sulfur	wood chip	600	Hg	320	2.0	57.8	107.5	Park et al. (2019)

3.12. Density functional theory (DFT) calculations

To interpret the adsorption behavior of cadmium (Cd) on biochar and sulfur-modified biochar, as well as the associated structural changes, Density Functional Theory (DFT) calculations were performed. DFT is a computational approach for modeling the electronic structure and properties of molecules and materials. In this study, DFT calculations were used to optimize the geometries of pristine and Cd-complexed forms of biochar and S-modified biochar. The optimized structures and energetics provide insights into the adsorption mechanisms, bonding interactions, and structural transformations during the Cd adsorption process.

The optimized structures displayed the hydrogen bonding distances between Cd and the biochar systems (Fig. 7). The Cd-S distance in the S-modified biochar complex was 2.9 Å, while the Cd-O bond length in the S-modified biochar reached 2.1 Å. Additionally, the Cd-O bond in the pristine biochar complex was 2.0 Å [SDB350-Cd]. The shorter Cd-O bond distance indicated a stronger interaction between Cd and oxygen functional groups in the S-modified biochar compared to undoped (pristine) biochar (Mamo et al., 2024). Moreover, the presence of sulfur in the S-modified biochar facilitated Cd interaction, as evidenced by the Cd-O bond formation and supported by the S atom which enhanced the electronic configuration and promoted the Cd-O bond, which is not available in the pristine biochar. Although the electrostatic interaction between Cd and sulfur is weak, the additional interaction between oxygen, sulfur and Cd contributed to the stability of the sulfur-modified biochar complex compared to the pristine system (Zhu et al., 2021). Additionally, the binding energies in the S-modified biochar-Cd complex were enhanced compared to pristine biochar (SDB350-Cd), reaching −55 kcal/mol versus −54 kcal/mol.

Furthermore, the electronic properties of the biochar systems were analyzed by evaluating the band gaps (Fig. S19, S20). For the interaction of Cd with pristine SDB350 biochar, forming the [SDB350-Cd] complex, the band gap was calculated to be 3.27 eV. This value is smaller than the band gap of 3.94 eV for the pristine SDB350, indicating that the presence of Cd alters the electronic structure of the unmodified biochar, likely influencing its reactivity and interactions with Cd (Tunalı et al., 2024).

On the other hand, the band gap for the sulfur-modified biochar complexed with Cd (S-modified biochar-Cd), representing the interaction of Cd with S-modified biochar, was 2.77 eV. This band gap value was more favorable compared to the band gap of 3.34 eV for the sulfur-modified biochar before Cd adsorption. The reduction in the band gap suggests that the interaction of Cd with sulfur-modified biochar facilitates charge transfer and enhances the electronic properties of the system, potentially contributing to improved Cd adsorption capabilities (Elgengehi et al., 2020).

A smaller band gap is more favorable for the interaction with Cd, explaining why the Cd interaction with sulfur-modified biochars showed higher Cd adsorption in a shorter time compared to the pristine biochar (SDB350), as the band gap was smaller in the case of the sulfur-modified

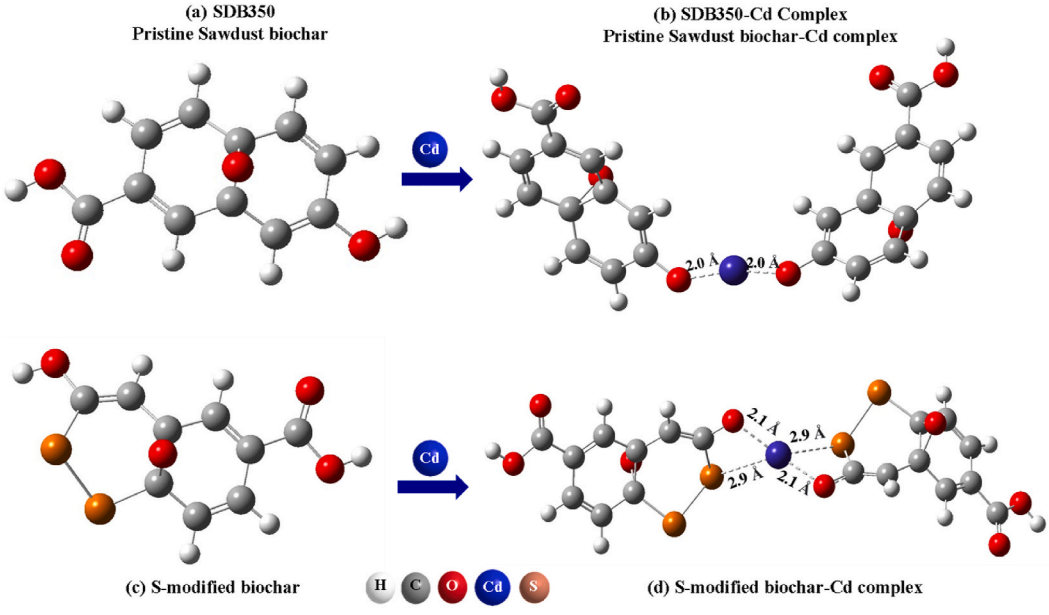

Fig. 7. Optimized molecular structures of biochar models and their cadmium complexes. (a) Pristine sawdust biochar (SDB350) (b) Pristine sawdust biochar-Cd complex [SDB350-Cd] (c) Sulfur-modified biochar (d) Sulfur-modified biochar-Cd complex [S-modified biochar-Cd]. All structures were optimized using density functional theory (DFT) at the B3LYP/LANL2DZ level of theory in the gas phase. Dashed lines indicate hydrogen bonds, with bond distances given in Ångstroms (Å).

biochar (Ghenaatian et al., 2019).

The analysis of band gaps provided visions into the electronic transitions and charge transfer processes occurring within the biochar-Cd complexes. The reduced band gaps observed for the [sulfur-modified biochar-Cd] and [SDB350-Cd] systems suggest that sulfur doping can modulate the electronic properties of biochar, potentially enhancing its adsorption capabilities and affinity towards Cd. These findings explicate the role of sulfur modifications in improving the Cd adsorption performance of biochar, complementing the experimental observations (Baachaoui et al., 2021; Oberoi et al., 2021).

3.13. Enhancing environmental remediation with sulfur-modified biochar from sustainable bioresources

This study highlights the potential of sulfur-modified biochar derived from sustainable bioresources, such as sawdust, for effective environmental applications. The modified biochar exhibits strong capabilities in adsorbing cadmium (Cd), a hazardous heavy metal, indicating its practical utility in remediating Cd-contaminated water and soil. These findings underscore the value of S-modified biochar as a sustainable and efficient material for the mitigation of heavy metal pollution. The simplicity and scalability of the S-modification process make it an attractive option for large-scale production of sulfur-functionalized biochar adsorbents, aligning with sustainable resource utilization principles. Beyond Cd, sulfur-containing functional groups integrated into biochar could broaden its adsorption capacity to include other soft acid pollutants like mercury and arsenic, supported by Pearson's Hard and Soft Acids and Bases (HSAB) theory and DFT. This versatility not only enhances environmental remediation efforts but also offers opportunities for the selective recovery of valuable metals from complex matrices, promoting resource conservation and sustainable material management practices in line with circular economy principles. Continued research optimizing bioresource utilization could further advance the development of cost-effective and environmentally friendly adsorbents tailored for specific contaminant removal applications, thereby contributing to the enhancement of environmental quality and human health protection.

4. Conclusions

This study demonstrates the efficacy of a simple chemical strategy for enhancing sawdust biochar's cadmium adsorption capacity through sulfur-doping. The incorporation of sulfur-based functional groups significantly improved surface functionality and adsorption performance, increasing Cd uptake by 4.8–9.0 times compared to pristine biochar. The synergistic interplay of multiple adsorption mechanisms, facilitated by both oxygen and sulfur functionalities, resulted in rapid equilibrium times and high adsorption capacities. Density Functional Theory calculations provided insights into the electronic modulation of biochar-Cd systems, viewing narrowed band gaps and enhanced stability of S-modified biochar-Cd complexes. These findings underscore the importance of tailored surface modifications in augmenting biochar's reactivity and affinity towards specific contaminants. The developed S-modified biochar presents an effective, sustainable, and potentially scalable solution for Cd removal from aqueous environments, contributing to advanced water treatment technologies and environmental remediation strategies. This research not only addresses the critical issue of heavy metal contamination but also aligns with circular economy principles by upcycling sawdust waste into high-value adsorbents. Future studies should focus on optimizing the sulfur-doping process, exploring its applicability to other heavy metals, and investigating the material's performance in real-world water treatment scenarios.

CRediT authorship contribution statement

M.M.M. Ahmed: Writing – review & editing, Writing – original draft, Visualization, Validation, Software, Methodology, Investigation, Formal analysis, Data curation, Conceptualization. **Chih-Hao Liao:** Visualization, Validation, Methodology, Investigation, Formal analysis, Data curation, Conceptualization. **S. Venkatesan:** Visualization, Validation, Software, Resources, Methodology, Investigation. **Yu-Ting Liu:** Validation, Supervision, Software, Resources, Project administration, Methodology, Investigation, Funding acquisition, Formal analysis, Data curation, Conceptualization. **Yu-Min Tzou:** Writing – review & editing, Visualization, Validation, Supervision, Software, Resources, Project administration, Methodology, Investigation, Funding acquisition, Formal analysis, Data curation, Conceptualization. **Shih-Hao Jien:** Visualization, Validation, Supervision, Software, Resources, Methodology, Investigation, Funding acquisition, Formal analysis, Data curation, Conceptualization. **Ming-Chang Lin:** Software, Resources, Project administration, Investigation, Funding acquisition, Formal analysis, Data curation. **Yi-Cheng Hsieh:** Validation, Software, Investigation, Data curation, Conceptualization. **Ahmed I. Osman:** Writing – review & editing, Visualization, Validation, Software, Resources, Methodology, Investigation, Data curation, Conceptualization.

Declaration of competing interest

The authors declare that they have no known competing financial interests or personal relationships that could have appeared to influence the work reported in this paper.

Acknowledgment

We extend our sincere appreciation to the Ministry of Science and Technology (MOST) for their financial support through project number 110-2313-B-005-023-MY. Additionally, this research was made possible by funding from the Ministry of Education (MOE) in Taiwan, specifically through the "Innovation and Development Center of Sustainable Agriculture" as part of the Featured Areas Research Center Program within the Higher Education Sprout Project framework.

Appendix A. Supplementary data

Supplementary data to this article can be found online at https://doi.org/10.1016/j.jenvman.2024.123586.

Data availability

Data will be made available on request.

References

Ahmed, M.M.M., Imae, T., Ohshima, H., Ariga, K., Shrestha, L.K., 2021. External magnetic field-enhanced supercapacitor performance of cobalt oxide/magnetic graphene composites. Bull. Chem. Soc. Jp. 94, 2245–2251. https://doi.org/10.1246/bcsj.20210222, 2021.

Ahmed, M.M.M., Liu, Y.-T., Venkatesan, S., Wu, M.C., Nail, H.M., Tzou, D.-L.M., Lin, M.-C., Chen, K.-Y., Tzou, Y.-m., 2023. Promotion of the catalytic polymerization of hydroquinone towards humic-like substances by graphitic carbon nitride. J. Environ. Chem. Eng. 11, 111026. https://doi.org/10.1016/j.jece.2023.111026.

Alkhadra, M.A., Su, X., Suss, M.E., Tian, H., Guyes, E.N., Shocron, A.N., Conforti, K.M., De Souza, J.P., Kim, N., Tedesco, M., 2022. Electrochemical methods for water purification, ion separations, and energy conversion. Chem. Rev. 122, 13547–13635. https://doi.org/10.1021/acs.chemrev.1c00396.

Amalina, F., Krishnan, S., Zularisam, A.W., Nasrullah, M., 2024. Pristine and modified biochar applications as multifunctional component towards sustainable future: recent advances and new insights. Sci. Total Environ. 914, 169608. https://doi.org/10.1016/j.scitotenv.2023.169608.

Baachaoui, S., Aldulaijan, S., Sementa, L., Fortunelli, A., Dhouib, A., Raouafi, N., 2021. Density functional theory investigation of graphene functionalization with activated carbenes and its application in the sensing of heavy metallic cations. J. Phys. Chem. C 125, 26418–26428. https://doi.org/10.1021/acs.jpcc.1c07247.

Bian, S., Shen, C., Hua, H., Zhou, L., Zhu, H., Xi, F., Liu, J., Dong, X., 2016. One-pot synthesis of sulfur-doped graphene quantum dots as a novel fluorescent probe for highly selective and sensitive detection of lead(ii). RSC Adv. 6 (74), 69977–69983. https://doi.org/10.1039/C6RA10836A.

Chang, P.-H., Mukhopadhyay, R., Sarkar, B., Mei, Y.-C., Hsu, C.-H., Tzou, Y.-M., 2023. Insight and mechanisms of tetracycline adsorption on sodium alginate/montmorillonite composite beads. App. Clay Sci. 245, 107127. https://doi.org/10.1016/j.clay.2023.107127.

Chaubey, A.K., Pratap, T., Preetiva, B., Patel, M., Singsit, J.S., Pittman Jr, C.U., Mohan, D., 2024. Definitive review of nanobiochar. ACS Omega 9, 12331–12379. https://doi.org/10.1021/acsomega.3c07804.

Chen, C.-N., Liao, C.-S., Tzou, Y.-M., Lin, Y.-T., Chang, E.-H., Jien, S.-H., 2024. Soil quality and microbial communities in subtropical slope lands under different agricultural management practices. Front. Microbio. 14, 1242217. https://doi.org/10.3389/fmicb.2023.1242217.

Chen, D., Wang, X., Wang, X., Feng, K., Su, J., Dong, J., 2020a. The mechanism of cadmium sorption by sulphur-modified wheat straw biochar and its application cadmium-contaminated soil. Sci. Total Environ. 714, 136550. https://doi.org/10.1016/j.scitotenv.2020.136550.

Chen, K.-Y., Liu, Y.-T., Hsieh, Y.-C., Tzou, Y.-M., 2020b. Organic fragments newly released from heat-treated peat soils create synergies with dissolved organic carbon to enhance Cr(VI) removal. Ecotox. Environ. Safety 201, 110800. https://doi.org/10.1016/j.ecoenv.2020.110800.

Chen, K.-Y., Tzou, Y.-M., Hsu, L.-C., Guo, J.-W., Cho, Y.-L., Teah, H.-Y., Hsieh, Y.-C., Liu, Y.-T., 2022. Oxidative removal of thallium (I) using Al beverage can waste with amendments of Fe: Tl speciation and removal mechanisms. Chem. Eng. J. 427, 130846. https://doi.org/10.1016/j.cej.2021.130846.

Chen, Q., Zheng, J., Zheng, L., Dang, Z., Zhang, L., 2018. Classical theory and electron-scale view of exceptional Cd(II) adsorption onto mesoporous cellulose biochar via experimental analysis coupled with DFT calculations. Chem. Eng. J. 350, 1000–1009. https://doi.org/10.1016/j.cej.2018.06.054.

Chen, R., Zhao, X., Jiao, J., Li, Y., Wei, M., 2019. Surface-modified biochar with polydentate binding sites for the removal of cadmium. Int. J. Molecul. Sci. 20, 1775. https://doi.org/10.3390/ijms20071775.

Chen, W., Yan, L., Bangal, P., 2010. Chemical reduction of graphene oxide to graphene by sulfur-containing compounds. J. Phys. Chem. C 114 (47), 19885–19890. https://doi.org/10.1021/jp107131v.

Cho, Y.-L., Lee, Y.-C., Hsu, L.-C., Wang, C.-C., Chen, P.-C., Liu, S.-L., Teah, H.-Y., Liu, Y.-T., Tzou, Y.-M., 2020. Molecular mechanisms for Pb removal by Cyanidiales: a potential biomaterial applied in thermo-acidic conditions. Chem. Eng. J. 401, 125828. https://doi.org/10.1016/j.cej.2020.125828.

Cowie, A., Azzi, E., Weng, Z.H., Woolf, D., 2024. Biochar, greenhouse gas accounting, and climate change mitigation. Biochar for Environmental Management 3rd Edition 759–784. https://doi.org/10.4324/9781003297673.

Curtiss, L.A., Redfern, P.C., Raghavachari, K., 2007. Gaussian-4 theory. J. Chem. Phys. 126 (8), 084108. https://doi.org/10.1063/1.2436888.

de Carvalho, E.F.V., Lopez-Castillo, A., Roberto-Neto, O., 2018. A comparative study of the structures and electronic properties of graphene fragments: a DFT and MP2 survey. Chem. Phys. Lett. 691, 291–297. https://doi.org/10.1016/j.cplett.2017.11.023.

de Falco, G., Li, W., Cimino, S., Bandosz, T.J., 2018. Role of sulfur and nitrogen surface groups in adsorption of formaldehyde on nanoporous carbons. Carbon 138, 283–291. https://doi.org/10.1016/j.carbon.2018.05.067.

Elgengehi, S.M., El-Taher, S., Ibrahim, M.A., Desmarais, J.K., El-Kelany, K.E., 2020. Graphene and graphene oxide as adsorbents for cadmium and lead heavy metals: a theoretical investigation. App. Surf. Sci. 507, 145038. https://doi.org/10.1016/j.apsusc.2019.145038.

Fan, J., Cai, C., Chi, H., Reid, B.J., Coulon, F., Zhang, Y., Hou, Y., 2020. Remediation of cadmium and lead polluted soil using thiol-modified biochar. J. Hazard Mater. 388, 122037. https://doi.org/10.1016/j.jhazmat.2020.122037.

Fawzy, S., Osman, A.I., Mehta, N., Moran, D., Al-Muhtaseb, A.a.H., Rooney, D.W., 2022. Atmospheric carbon removal via industrial biochar systems: a techno-economic-environmental study. J. Clean. Prod. 371, 133660. https://doi.org/10.1016/j.jclepro.2022.133660.

Fawzy, S., Osman, A.I., Yang, H., Doran, J., Rooney, D.W., 2021. Industrial biochar systems for atmospheric carbon removal: a review. Environ. Chem. Lett. 19, 3023–3055. https://doi.org/10.1007/s10311-021-01210-1.

Gariganti, N., Pagadala, E., Loke, S.K., Javisetti, A., Poola, B., Sharif, S.M., Srinivasadesikan, V., Katari, N.K., Kottalanka, R.K., 2024. Design, synthesis and apoptotic activity of substituted chalcones tethered 1,3,5-triazine hybrids: an insights from molecular docking, molecular dynamics simulations, DFT, ADME, and DAPI analyses. J. Molecul. Struct. 138869. https://doi.org/10.1016/j.molstruc.2024.138869.

Geissler, C.H., Maravelias, C.T., 2022. Analysis of alternative bioenergy with carbon capture strategies: present and future. Energy Environ. Sci. 15, 2679–2689. https://doi.org/10.1039/D2EE00625A.

Ghenaatian, H.R., Shakourian-Fard, M., Kamath, G., 2019. The effect of sulfur and nitrogen/sulfur co-doping in graphene surface on the adsorption of toxic heavy metals (Cd, Hg, Pb). J. Mater. Sci. 54, 13175–13189. https://doi.org/10.1007/s10853-019-03791-3.

He, D., Luo, Y., Zhu, B., 2024. Feedstock and pyrolysis temperature influence biochar properties and its interactions with soil substances: insights from a DFT calculation. Sci. Total Environ. 922, 171259. https://doi.org/10.1016/j.scitotenv.2024.171259.

He, X., Hong, Z.-n., Jiang, J., Dong, G., Liu, H., Xu, R.-k., 2021. Enhancement of Cd (II) adsorption by rice straw biochar through oxidant and acid modifications. Environ. Sci. Pollut. Res. 28, 42787–42797. https://doi.org/10.1007/s11356-021-13742-8.

Ho, T.-L., 1975. Hard soft acids bases (HSAB) principle and organic chemistry. Chem. Rev. 75 (1), 1–20. https://doi.org/10.1021/cr60293a001.

Hua, K., Xu, X., Luo, Z., Fang, D., Bao, R., Yi, J., 2020. Effective removal of mercury ions in aqueous solutions: a review. Current Nanosci 16, 363–375. https://doi.org/10.2174/1573413715666190112110659.

Huang, X., Guida, S., Jefferson, B., Soares, A., 2020. Economic evaluation of ion-exchange processes for nutrient removal and recovery from municipal wastewater. NPJ Clean Water 3, 1–10. https://doi.org/10.1038/s41545-020-0054-x.

Huangmee, K., Hsu, L.-C., Tzou, Y.-M., Cho, Y.-L., Liao, C.-H., Teah, H.Y., Liu, Y.-T., 2024. Thiol-functionalized black carbon as effective and economical materials for Cr (VI) removal: simultaneous sorption and reduction. J. Environ. Manag. 360, 121074. https://doi.org/10.1016/j.jenvman.2024.121074.

Hwang, J.-J., Hu, F.-H., Li, M.-X., Luo, K.-H., Liu, Y.-H., Lin, S.-R., Yeh, J.-M., 2024. Superhydrophobic surface of biomass carbon-based PANI composite coatings with the biomimetic structure of goose feather for anticorrosion/antibiofilm applications. Surf. Coat. Tech. 130700. https://doi.org/10.1016/j.surfcoat.2024.130700.

Kainth, S., Sharma, P., Pandey, O., 2024. Green sorbents from agricultural wastes: a review of sustainable adsorption materials. App. Surf. Sci. Adv. 19, 100562. https://doi.org/10.1016/j.apsadv.2023.100562.

Khan, R., Shukla, S., Kumar, M., Zuorro, A., Pandey, A., 2023. Sewage sludge derived biochar and its potential for sustainable environment in circular economy: advantages and challenges. Chem. Eng. J. 144495. https://doi.org/10.1016/j.cej.2023.144495.

Khan, Z.H., Gao, M., Qiu, W., Song, Z., 2020. Properties and adsorption mechanism of magnetic biochar modified with molybdenum disulfide for cadmium in aqueous solution. Chemosphere 255, 126995. https://doi.org/10.1016/j.chemosphere.2020.126995.

Khin, M.M., Nair, A.S., Babu, V.J., Murugan, R., Ramakrishna, S., 2012. A review on nanomaterials for environmental remediation. Energy Environ. Sci. 5, 8075–8109. https://doi.org/10.1039/C2EE21818F.

Kim, S., Nam, S.-N., Jang, A., Jang, M., Park, C.M., Son, A., Her, N., Heo, J., Yoon, Y., 2022. Review of adsorption–membrane hybrid systems for water and wastewater treatment. Chemosphere 286, 131916. https://doi.org/10.1016/j.chemosphere.2021.131916.

Kurniawan, T.A., Othman, M.H.D., Liang, X., Goh, H.H., Gikas, P., Chong, K.-K., Chew, K. W., 2023. Challenges and opportunities for biochar to promote circular economy and carbon neutrality. J. Environ. Manag. 332, 117429. https://doi.org/10.1016/j.jenvman.2023.117429.

Lee, J.W., Hawkins, B., Day, D.M., Reicosky, D.C., 2010. Sustainability: the capacity of smokeless biomass pyrolysis for energy production, global carbon capture and sequestration. Energy Environ. Sci. 3, 1695–1705. https://doi.org/10.1039/C004561F.

Leng, L., Liu, R., Xu, S., Mohamed, B.A., Yang, Z., Hu, Y., Chen, J., Zhao, S., Wu, Z., Peng, H., Li, H., Li, H., 2022. An overview of sulfur-functional groups in biochar from pyrolysis of biomass. J. Environ. Chem. Eng. 10, 107185. https://doi.org/10.1016/j.jece.2022.107185.

Li, Q., Liang, N., Zou, W., Han, X., Chang, C., Chen, J., 2024. Nitrogen-doped activated carbon derived from biomass waste for effective removal of doxycycline from aqueous solution: characterization and adsorption mechanism. J. Porous Mater. 1–14. https://doi.org/10.1007/s10934-024-01612-w.

Li, W.-H., Hsu, L.-C., Tzou, Y.-M., Chen, Y.-C., Teah, H.Y., Kung, Y.-Y., Chen, H.-Y., Liu, Y.-T., 2023. Hybridize magnesium-iron layered double hydroxide with biopolymers to develop multiple pathways for phosphate sorption and release: a potential slow release phosphorus fertilizer. Chem. Eng. J. 473, 145451. https://doi.org/10.1016/j.cej.2023.145451.

Lin, C.-C., Liu, Y.-T., Chang, P.-H., Hsieh, Y.-C., Tzou, Y.-M., 2023. Inhibition of continuous cropping obstacle of celery by chemically modified biochar: an efficient approach to decrease bioavailability of phenolic allelochemicals. J. Environ. Manag. 348, 119316. https://doi.org/10.1016/j.jenvman.2023.119316.

Liu, M., Almatrafi, E., Zhang, Y., Xu, P., Song, B., Zhou, C., Zeng, G., Zhu, Y., 2022a. A critical review of biochar-based materials for the remediation of heavy metal contaminated environment: applications and practical evaluations. Sci. Total Environ. 806, 150531. https://doi.org/10.1016/j.scitotenv.2021.150531.

Liu, T., Lawluvy, Y., Shi, Y., Ighalo, J.O., He, Y., Zhang, Y., Yap, P.-S., 2022b. Adsorption of cadmium and lead from aqueous solution using modified biochar: a review. J. Environ. Chem. Eng. 10, 106502. https://doi.org/10.1016/j.jece.2021.106502.

Liu, W.-J., Jiang, H., Yu, H.-Q., 2019. Emerging applications of biochar-based materials for energy storage and conversion. Energy Environ. Sci. 12, 1751–1779. https://doi.org/10.1039/C9EE00206E.

Lopez-Ramon, M.V., Stoeckli, F., Moreno-Castilla, C., Carrasco-Marin, F., 1999. On the characterization of acidic and basic surface sites on carbons by various techniques. Carbon 37, 1215–1221. https://doi.org/10.1016/S0008-6223(98)00317-0.

Luo, L., Wang, J., Lv, J., Liu, Z., Sun, T., Yang, Y., Zhu, Y.-G., 2023. Carbon sequestration strategies in soil using biochar: advances, challenges, and opportunities. Environ. Sci. Tech. 57, 11357–11372. https://doi.org/10.1021/acs.est.3c02620.

Ma, F., Zhao, H., Zheng, X., Zhao, B., Diao, J., Jiang, Y., 2023. Enhanced adsorption of cadmium from aqueous solution by amino modification biochar and its adsorption mechanism insight. J. Environ. Chem. Eng. 11, 109747. https://doi.org/10.1016/j.jece.2023.109747.

Ma, R., Xu, X., Zhang, Y., Zhang, D., Xiang, G., Chen, Y., Qian, J., Yi, S., 2024. Synergistic effects of adsorption and chemical reduction towards the effective Cr(VI) removal in the presence of the sulfur-doped biochar material. Environ. Sci. Pollut. Res. Int. 31, 8538–8551. https://doi.org/10.1007/s11356-023-31654-7.

Majumder, S., Sharma, P., Singh, S.P., Nadda, A.K., Sahoo, P.K., Xia, C., Sharma, S., Ganguly, R., Lam, S.S., Kim, K.H., 2023. Engineered biochar for the effective sorption and remediation of emerging pollutants in the environment. J. Environ. Chem. Eng. 11, 109590. https://doi.org/10.1016/j.jece.2023.109590.

Mamo, T.T., Qorbani, M., Hailemariam, A.G., Putikam, R., Chu, C.-M., Ko, T.-R., Sabbah, A., Huang, C.-Y., Kholimatussadiah, S., Billo, T., Hussien, M.K., Chang, S.-Y., Lin, M.-C., Woon, W.-Y., Wu, H.-L., Wong, K.-T., Chen, L.-C., Chen, K.-H., 2024. Enhanced CO_2 photoreduction to CH_4 via *COOH and *CHO intermediates stabilization by synergistic effect of implanted P and S vacancy in thin-film SnS_2. Nano Energy 128, 109863. https://doi.org/10.1016/j.nanoen.2024.109863.

Mishra, R.K., Kumar, D.J.P., Narula, A., Chistie, S.M., Naik, S.U., 2023. Production and beneficial impact of biochar for environmental application: a review on types of feedstocks, chemical compositions, operating parameters, techno-economic study, and life cycle assessment. Fuel 343, 127968. https://doi.org/10.1016/j.fuel.2023.127968.

Narmadha, V., Sreemahadevan, S., 2024. Plant-based biosorbents for heavy metal removal from wastewater. Sustainable Machining Green Manufacturing 155–176. https://doi.org/10.1002/9781394197866.ch8.

O'Connor, D., Peng, T., Li, G., Wang, S., Duan, L., Mulder, J., Cornelissen, G., Cheng, Z., Yang, S., Hou, D., 2018. Sulfur-modified rice husk biochar: a green method for the remediation of mercury contaminated soil. Sci. Total Environ. 621, 819–826. https://doi.org/10.1016/j.scitotenv.2017.11.213.

Oberoi, A.S., Huang, H., Khanal, S.K., Sun, L., Lu, H., 2021. Electron distribution in sulfur-driven autotrophic denitrification under different electron donor and acceptor feeding schemes. Chem. Eng. J. 404, 126486. https://doi.org/10.1016/j.cej.2020.126486.

Osman, A.I., Farghali, M., Rashwan, A.K., 2024. Life cycle assessment of biochar as a green sorbent for soil remediation. Current Opin. Green Sustain. Chem. 46, 100882. https://doi.org/10.1016/j.cogsc.2024.100882.

Osman, A.I., Fawzy, S., Farghali, M., El-Azazy, M., Elgarahy, A.M., Fahim, R.A., Maksoud, M.I.A.A., Ajlan, A.A., Yousry, M., Saleem, Y., Rooney, D.W., 2022. Biochar for agronomy, animal farming, anaerobic digestion, composting, water treatment, soil remediation, construction, energy storage, and carbon sequestration: a review. Environ. Chem. Lett. 20, 2385–2485. https://doi.org/10.1007/s10311-022-01424-x.

Osman, A.I., Lai, Z.Y., Farghali, M., Yiin, C.L., Elgarahy, A.M., Hammad, A., Ihara, I., Al-Fatesh, A.S., Rooney, D.W., Yap, P.-S., 2023a. Optimizing biomass pathways to bioenergy and biochar application in electricity generation, biodiesel production, and biohydrogen production. Environ. Chem. Lett. 21, 2639–2705. https://doi.org/10.1007/s10311-023-01613-2.

Osman, A.I., Zhang, Y., Lai, Z.Y., Rashwan, A.K., Farghali, M., Ahmed, A.A., Liu, Y., Fang, B., Chen, Z., Al-Fatesh, A., Rooney, D.W., Yiin, C.L., Yap, P.-S., 2023b. Machine learning and computational chemistry to improve biochar fertilizers: a review. Environ. Chem. Lett. 21, 3159–3244. https://doi.org/10.1007/s10311-023-01631-0.

Ostermeyer, P., Bonin, L., Folens, K., Verbruggen, F., García-Timermans, C., Verbeken, K., Rabaey, K., Hennebel, T., 2021. Effect of speciation and composition on the kinetics and precipitation of arsenic sulfide from industrial metallurgical wastewater. J. Hazard Mater. 409, 124418. https://doi.org/10.1016/j.jhazmat.2020.124418.

Park, J.-H., Wang, J.J., Zhou, B., Mikhael, J.E., DeLaune, R.D., 2019. Removing mercury from aqueous solution using sulfurized biochar and associated mechanisms. Environ. Pollut. 244, 627–635. https://doi.org/10.1016/j.envpol.2018.10.069.

Pearson, R.G., Songstad, J., 1967. Application of the principle of hard and soft acids and bases to organic chemistry. J. Am. Chem. Soc. 89, 1827–1836. https://doi.org/10.1021/ja00984a014.

Petrovic, B., Gorbounov, M., Masoudi Soltani, S., 2022. Impact of surface functional groups and their introduction methods on the mechanisms of CO_2 adsorption on porous carbonaceous adsorbents. carbon capture Sci. Tech. 3, 100045. https://doi.org/10.1016/j.ccst.2022.100045.

Phuong, D.T., Loc, N.X., 2022. Rice straw biochar and magnetic rice straw biochar for Safranin O adsorption from aqueous solution. Water 14 (2), 186. https://doi.org/10.3390/w14020186.

Rafiq, S., Wongrod, S., Vinitnantharat, S., 2023. Adsorption kinetics of cadmium and lead by biochars in single- and bisolute brackish water systems. ACS Omega 8, 45262–45276. https://doi.org/10.1021/acsomega.3c03335.

Rajendran, S., Priya, A., Kumar, P.S., Hoang, T.K., Sekar, K., Chong, K.Y., Khoo, K.S., Ng, H.S., Show, P.L., 2022. A critical and recent developments on adsorption technique for removal of heavy metals from wastewater-A review. Chemosphere 303, 135146. https://doi.org/10.1016/j.chemosphere.2022.135146.

Shen, Y.-S., Wang, S.-L., Tzou, Y.-M., Yan, Y.-Y., Kuan, W.-H., 2012. Removal of hexavalent Cr by coconut coir and derived chars–the effect of surface functionality. Bioresour. Tech. 104, 165–172. https://doi.org/10.1016/j.biortech.2011.10.096.

Sovacool, B.K., Del Rio, D.F., Herman, K., Iskandarova, M., Uratani, J.M., Griffiths, S., 2024. Reconfiguring European industry for net-zero: a qualitative review of hydrogen and carbon capture utilization and storage benefits and implementation challenges. Energy Environ. Sci. 17, 3523–3569. https://doi.org/10.1039/D3EE03270A.

Tunalı, Ö.F., Yuksel, N., Gece, G., Fellah, M.F., 2024. A DFT study of H_2S adsorption and sensing on Ti, V, Cr and Sc doped graphene surfaces. Struct. Chem. 1–17. https://doi.org/10.1007/s11224-023-02265-2.

Tyagi, U., Anand, N., 2023. Prospective of waste lignocellulosic biomass as precursors for the production of biochar: application, performance, and mechanism—a Review. BioEnergy Res. 16, 1335–1360. https://doi.org/10.1007/s12155-022-10560-9.

Vijayakumar, S., Raja, L., Venkatesan, S., Lin, M.-C., Vediappen, P., 2024. A Highly selective Schiff base based chemodosimeter for the detection of perfluorooctanoic acid by optical biosensor. J. Fluoresc. 34, 787–794. https://doi.org/10.1007/s10895-023-03298-w.

Wan, Y., Hu, Y., Zhou, W., 2022. Catalytic mechanism of nitrogen-doped biochar under different pyrolysis temperatures: the crucial roles of nitrogen incorporation and carbon configuration. Sci. Total Environ. 816, 151502. https://doi.org/10.1016/j.scitotenv.2021.151502.

Wang, S., Sheng, Y., Feng, M., Leszczynski, J., Wang, L., Tachikawa, H., Yu, H., 2007. Light-induced cytotoxicity of 16 polycyclic aromatic hydrocarbons on the US EPA priority pollutant list in human skin HaCaT keratinocytes: relationship between phototoxicity and excited state properties. Environ. Toxicol.: Int. J. 22, 318–327. https://doi.org/10.1002/tox.20241.

Wang, Z., Lu, Q., Liu, C., Tian, H., Wang, J., Xie, L., Liu, Q., Zeng, H., 2024. Nanoscale insights into the interaction mechanism underlying the adsorption and retention of heavy metal ions by humic acid. Environm. Sci. Tech. 58, 3412–3422. https://doi.org/10.1021/acs.est.3c08309.

Xia, H., Zhang, Y., Chen, Q., Liu, R., Wang, H., 2023. Unraveling adsorption characteristics and removal mechanism of novel Zn/Fe-bimetal-loaded and starch-coated corn cobs biochar for Pb(II) and Cd(II) in wastewater. J. Molecul. Liq. 391, 123375. https://doi.org/10.1016/j.molliq.2023.123375.

Yang, X., Jiang, D., Cheng, X., Yuan, C., Wang, S., He, Z., Esakkimuthu, S., 2022. Adsorption properties of seaweed-based biochar with the greenhouse gases (CO_2, CH_4, N_2O) through density functional theory (DFT). Biomass Bioenergy 163, 106519. https://doi.org/10.1016/j.biombioe.2022.106519.

Yin, K., Wang, J., Zhai, S., Xu, X., Li, T., Sun, S., Xu, S., Zhang, X., Wang, C., Hao, Y., 2022a. Adsorption mechanisms for cadmium from aqueous solutions by oxidant-modified biochar derived from Platanus orientalis Linn leaves. J. Hazard Mater. 428, 128261. https://doi.org/10.1016/j.jhazmat.2022.128261.

Yin, M., Bai, X., Wu, D., Li, F., Jiang, K., Ma, N., Chen, Z., Zhang, X., Fang, L., 2022b. Sulfur-functional group tunning on biochar through sodium thiosulfate modified molten salt process for efficient heavy metal adsorption. Chem. Eng. J. 433, 134441. https://doi.org/10.1016/j.cej.2021.134441.

Yu, H., Zhang, Y., Wang, L., Tuo, Y., Yan, S., Ma, J., Zhang, X., Shen, Y., Guo, H., Han, L., 2024. Experimental and DFT insights into the adsorption mechanism of methylene blue by alkali-modified corn straw biochar. RSC Adv. 14, 1854–1865. https://doi.org/10.1039/D3RA05964B.

Yuan, X., Cao, Y., Li, J., Patel, A.K., Dong, C.-D., Jin, X., Gu, C., Yip, A.C.K., Tsang, D.C.W., Ok, Y.S., 2023. Recent advancements and challenges in emerging applications of biochar-based catalysts. Biotech. Adv 67, 108181. https://doi.org/10.1016/j.biotechadv.2023.108181.

Zhang, K., Chen, Y., Fang, Z., 2023a. Highly efficient removal of cadmium by sulfur-modified biochar: process and mechanism. Water, Air, Soil Pollut. 234, 26. https://doi.org/10.1007/s11270-022-06005-w.

Zhang, L., Zhang, T., Cai, Y., Zhao, Y., Song, S., Quintana, M., 2023b. Engineering sulfuric acid-pretreated biochar supporting MnO_2 for efficient toxic organic pollutants removal from aqueous solution in a wide pH range. J. Clean. Prod. 416, 137968. https://doi.org/10.1016/j.jclepro.2023.137968.

Zhang, P., Duan, W., Peng, H., Pan, B., Xing, B., 2022. Functional biochar and its balanced design. ACS Environ. Au 2, 115–127. https://doi.org/10.1021/acsenvironau.1c00032.

Zhao, B., O'Connor, D., Zhang, J., Peng, T., Shen, Z., Tsang, D.C., Hou, D., 2018. Effect of pyrolysis temperature, heating rate, and residence time on rapeseed stem derived biochar. J. Clean. Prod. 174, 977–987. https://doi.org/10.1016/j.jclepro.2017.11.013.

Zhao, W., Tan, P., Zhang, J., Liu, J., 2010. Charge transfer and optical phonon mixing in few-layer graphene chemically doped with sulfuric acid. Phys. Rev.B—Condensed Matter Mater. Phys. 82 (24), 245423. https://doi.org/10.1103/PhysRevB.82.245423.

Zhao, W., Zhang, Z., Xin, Y., Xiao, R., Gao, F., Wu, H., Wang, W., Guan, Q., Lu, K., 2024. Na_2S-modified biochar for Hg (II) removal from wastewater: a techno-economic assessment. Fuel 356, 129641. https://doi.org/10.1016/j.fuel.2023.129641.

Zhou, Y., Yang, Y., Liu, G., He, G., Liu, W., 2020. Adsorption mechanism of cadmium on microplastics and their desorption behavior in sediment and gut environments: the roles of water pH, lead ions, natural organic matter and phenanthrene. Water Res. 184, 116209. https://doi.org/10.1016/j.watres.2020.116209.

Zhu, L., Tong, L., Zhao, N., Wang, X., Yang, X., Lv, Y., 2020a. Key factors and microscopic mechanisms controlling adsorption of cadmium by surface oxidized and aminated biochars. J. Hazard Mater. 382, 121002. https://doi.org/10.1016/j.jhazmat.2019.121002.

Zhu, Y., Liang, H., Yu, R., Hu, G., Chen, F., 2020b. Removal of aquatic cadmium ions using thiourea modified poplar biochar. Water 12, 1117. https://doi.org/10.3390/w12041117.

Zhu, Z., Liu, Z., Tang, X., Reeti, K., Huo, P., Wong, J.W.-C., Zhao, J., 2021. Sulfur-doped g-C_3N_4 for efficient photocatalytic CO_2 reduction: insights by experiment and first-principles calculations. Catal. Sci. Tech. 11, 1725–1736. https://doi.org/10.1039/D0CY02382E.